Title

Study of the production of charged pions, kaons, and protons in pPb collisions at sNN=5.02TeV

Journal

European Physical Journal C, 74(6)

ISSN

1434-6044

Authors

The CMS Collaboration

Chatrchyan, S

Khachatryan, V

et al.

Publication Date

2014-06-01

DOI

10.1140/epjc/s10052-014-2847-x

Eur. Phys. J. C (2014) 74:2847
DOI 10.1140/epjc/s10052-014-2847-x

THE EUROPEAN PHYSICAL JOURNAL C

Regular Article - Experimental Physics

Study of the production of charged pions, kaons, and protons in pPb collisions at $\sqrt{s_{NN}} = 5.02$ TeV

The CMS Collaboration[⋆]

CERN, Geneva, Switzerland

Received: 12 July 2013 / Accepted: 4 April 2014 / Published online: 3 June 2014

Abstract Spectra of identified charged hadrons are measured in pPb collisions with the CMS detector at the LHC at $\sqrt{s_{NN}} = 5.02$ TeV. Charged pions, kaons, and protons in the transverse-momentum range $p_{\mathrm{T}} \approx 0.1$–$1.7$ GeV/c and laboratory rapidity $|y| < 1$ are identified via their energy loss in the silicon tracker. The average p_{T} increases with particle mass and the charged multiplicity of the event. The increase of the average p_{T} with charged multiplicity is greater for heavier hadrons. Comparisons to Monte Carlo event generators reveal that EPOS LHC, which incorporates additional hydrodynamic evolution of the created system, is able to reproduce most of the data features, unlike HIJING and AMPT. The p_{T} spectra and integrated yields are also compared to those measured in pp and PbPb collisions at various energies. The average transverse momentum and particle ratio measurements indicate that particle production at LHC energies is strongly correlated with event particle multiplicity.

1 Introduction

The study of hadron production has a long history in high-energy particle and nuclear physics, as well as in cosmic-ray physics. The absolute yields and the transverse momentum (p_{T}) spectra of identified hadrons in high-energy hadron–hadron collisions are among the most basic physical observables. They can be used to test the predictions for non-perturbative quantum chromodynamics (QCD) processes like hadronization and soft-parton interactions, and the validity of their implementation in Monte Carlo (MC) event generators. Spectra of identified particles in proton–nucleus collisions also constitute an important reference for studies of high-energy heavy-ion collisions, where final-state effects are known to modify the spectral shape and yields of different hadron species [1–7].

The present analysis focuses on the measurement of the p_{T} spectra of charged hadrons, identified mostly via their energy deposits in silicon detectors, in pPb collisions at $\sqrt{s_{NN}} = 5.02$ TeV. The analysis procedures are similar to those previously used in the measurement of pion, kaon, and proton production in pp collisions at several center-of-mass energies [8]. Results on π, K, and p production in pPb collisions have been also reported by the ALICE Collaboration [9].

A detailed description of the CMS (Compact Muon Solenoid) detector can be found in Ref. [10]. The CMS experiment uses a right-handed coordinate system, with the origin at the nominal interaction point (IP) and the z axis along the counterclockwise-beam direction. The pseudorapidity η and rapidity y of a particle (in the laboratory frame) with energy E, momentum p, and momentum along the z axis p_z are defined as $\eta = -\ln[\tan(\theta/2)]$, where θ is the polar angle with respect to the z axis and $y = \frac{1}{2}\ln[(E + p_z)/(E - p_z)]$, respectively. The central feature of the CMS apparatus is a superconducting solenoid of 6 m internal diameter. Within the 3.8 T field volume are the silicon pixel and strip tracker, the crystal electromagnetic calorimeter, and the brass/scintillator hadron calorimeter. The tracker measures charged particles within the pseudorapidity range $|\eta| < 2.4$. It has 1440 silicon pixel and 15 148 silicon strip detector modules, ordered in 13 tracking layers in the y region studied here. In addition to the barrel and endcap detectors, CMS has extensive forward calorimetry. Steel/quartz-fiber forward calorimeters (HF) cover $3 < |\eta| < 5$. Beam Pick-up Timing for the eXperiments (BPTX) devices were used to trigger the detector readout. They are located around the beam pipe at a distance of 175 m from the IP on either side, and are designed to provide precise information on the Large Hadron Collider (LHC) bunch structure and timing of the incoming beams.

The reconstruction of charged particles in CMS is bounded by the acceptance of the tracker ($|\eta| < 2.4$) and by the decreasing tracking efficiency at low momentum (greater than about 60 % for $p > 0.05$, 0.10, 0.20, and 0.40 GeV/c for e, π, K, and p, respectively). Particle identification capabilities using specific ionization are restricted to $p < 0.15$ GeV/c for electrons, $p < 1.20$ GeV/c for pions, $p < 1.05$ GeV/c

⋆ e-mail: cms-publication-committee-chair@cern.ch

for kaons, and $p < 1.70\,\text{GeV}/c$ for protons. Pions are identified up to a higher momentum than kaons because of their high relative abundance. In view of the (y, p_T) regions where pions, kaons, and protons can all be identified ($p = p_\text{T} \cosh y$), the band $-1 < y < 1$ (in the laboratory frame) was chosen for this measurement, since it is a good compromise between the p_T range and y coverage.

In this paper, comparisons are made to predictions from three MC event generators. The HIJING [11] event generator is based on a two-component model for hadron production in high-energy nucleon and nuclear collisions. Hard parton scatterings are assumed to be described by perturbative QCD and soft interactions are approximated by string excitations with an effective cross section. In version 2.1 [12], in addition to modification of initial parton distributions, multiple scatterings inside a nucleus lead to transverse momentum broadening of both initial and final-state partons. This is responsible for the enhancement of intermediate-p_T (2–6 GeV/c) hadron spectra in proton–nucleus collisions, with respect to the properly scaled spectra of proton–proton collisions (Cronin effect). The AMPT [13] event generator is a multi-phase transport model. It starts from the same initial conditions as HIJING, contains a partonic transport phase, the description of the bulk hadronization, and finally a hadronic rescattering phase. These processes lead to hydrodynamic-like effects in simulated nucleus–nucleus collisions, but not necessarily in proton–nucleus collisions. The latest available version (1.26/2.26) is used. The EPOS [14] event generator uses a quantum mechanical multiple scattering approach based on partons and strings, where cross sections and particle production are calculated consistently, taking into account energy conservation in both cases. Nuclear effects related to transverse momentum broadening, parton saturation, and screening have been introduced. The model can be used both for extensive air shower simulations and accelerator physics. EPOS LHC [15] is an improvement of version 1.99 (v3400) and contains a three-dimensional viscous event-by-event hydrodynamic treatment. This is a major difference with respect to the HIJING and AMPT models for proton–nucleus collisions.

2 Data analysis

The data were taken in September 2012 during a 4-h-long pPb run with very low probability of multiple interactions (0.15 % "pileup"). A total of 2.0 million collisions were collected, corresponding to an integrated luminosity of approximately $1\,\mu\text{b}^{-1}$. The dominant uncertainty for the reported measurements is systematic in nature. The beam energies were 4 TeV for protons and 1.58 TeV per nucleon for lead nuclei, resulting in a center-of-mass energy per nucleon pair of $\sqrt{s_{NN}} = 5.02$ TeV. Due to the asymmetric beam energies the nucleon-nucleon center-of-mass in the pPb collisions was not at rest with respect to the laboratory frame but was moving with a velocity $\beta = -0.434$ or rapidity -0.465. Since the higher-energy proton beam traveled in the clockwise direction, i.e. at $\theta = \pi$, the rapidity of a particle emitted at y_cm in the nucleon-nucleon center-of-mass frame is detected in the laboratory frame with a shift, $y - y_\text{cm} = -0.465$, i.e. a particle with $y = 0$ moves with rapidity 0.465 in the Pb-beam direction in the center-of-mass system. The particle yields reported in this paper have been measured for laboratory rapidity $|y| < 1$ to match the experimentally accessible region.

The event selection consisted of the following requirements:

- at the trigger level, the coincidence of signals from both BPTX devices, indicating the presence of both proton and lead bunches crossing the interaction point; in addition, at least one track with $p_\text{T} > 0.4\,\text{GeV}/c$ in the pixel tracker;
- offline, the presence of at least one tower with energy above 3 GeV in each of the HF calorimeters; at least one reconstructed interaction vertex; beam-halo and beam-induced background events, which usually produce an anomalously large number of pixel hits [16], are suppressed.

The efficiencies for event selection, tracking, and vertexing were evaluated using simulated event samples produced with the HIJING 2.1 MC event generator, where the CMS detector response simulation was based on GEANT4 [17]. Simulated events were reconstructed in the same way as collision data events. The final results were corrected to a particle level selection applied to the direct MC output, which is very similar to the data selection described above: at least one particle (proper lifetime $\tau > 10^{-18}$ s) with $E > 3$ GeV in the range $-5 < \eta < -3$ and at least one in the range $3 < \eta < 5$; this selection is referred to in the following as the "double-sided" (DS) selection. These requirements are expected to suppress single-diffractive collisions in both the data and MC samples. From the MC event generators studied in this paper, the DS selection efficiency for inelastic, hadronic collisions is found to be 94–97 %.

The simulated ratio of the data selection efficiency to the DS selection efficiency is shown as a function of the reconstructed track multiplicity in the top panel of Fig. 1. The ratio is used to correct the measured events. The results are also corrected for the fraction of DS events without a reconstructed track. This fraction, as given by the simulation, is about 0.1 %.

The extrapolation of particle spectra into the unmeasured (y, p_T) regions is model dependent, particularly at low p_T. A high-precision measurement therefore requires reliable track reconstruction down to the lowest possible p_T. The present analysis extends to $p_\text{T} \approx 0.1\,\text{GeV}/c$ by exploiting special

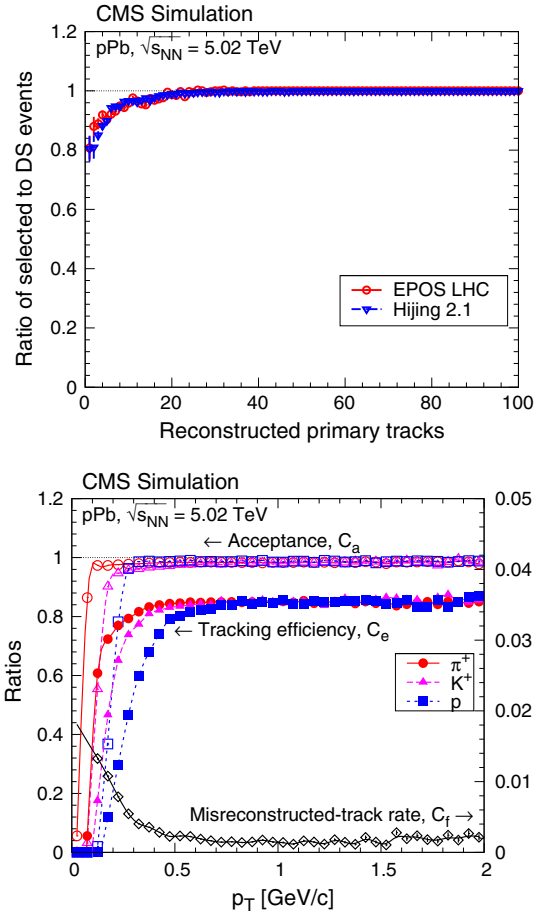

Fig. 1 *Top* the ratio of selected events to double-sided (DS) events (ratio of the corresponding efficiencies in the inelastic sample), according to EPOS LHC and HIJING MC simulations, as a function of the reconstructed primary charged-particle multiplicity. *Bottom* acceptance, tracking efficiency (*left* scale), and misreconstructed-track rate (*right* scale) in the range $|\eta| < 2.4$ as a function of p_{T} for positively charged pions, kaons, and protons

tracking algorithms [18], used in previous studies [8,16,19], to provide high reconstruction efficiency and low background rate. The charged-pion mass was assumed when fitting particle momenta.

The acceptance of the tracker (C_{a}) is defined as the fraction of primary charged particles leaving at least two hits in the pixel detector. It is flat in the region $-2 < \eta < 2$ and $p_{\mathrm{T}} > 0.4\,\mathrm{GeV}/c$, and its value is 96–98 % (Fig. 1, bottom panel). The loss of acceptance at $p_{\mathrm{T}} < 0.4\,\mathrm{GeV}/c$ is caused by energy loss and multiple scattering of particles, both depending on the particle mass. Likewise, the reconstruction efficiency (C_{e}) is about 75–85 %, degrading at low p_{T}, also in a mass-dependent way. The misreconstructed-track rate (C_f) is very small, reaching 1 % only for $p_{\mathrm{T}} < 0.2\,\mathrm{GeV}/c$. The probability of reconstructing multiple tracks (C_{m}) from a single true track is about 0.1 %, mostly due to particles spiralling in the strong magnetic field of the CMS solenoid. The efficiencies and background rates do not depend on the charged-multiplicity of the event. They largely factorize in η and p_{T}, but for the final corrections an (η, p_{T}) matrix is used.

The region where pPb collisions occur (beam spot) is measured by reconstructing vertices from many events. Since the bunches are very narrow in the transverse direction, the xy location of the interaction vertices is well constrained; conversely, their z coordinates are spread over a relatively long distance and must be determined on an event-by-event basis. The vertex position is determined using reconstructed tracks which have $p_{\mathrm{T}} > 0.1\,\mathrm{GeV}/c$ and originate from the vicinity of the beam spot, i.e. their transverse impact parameters d_{T} satisfy the condition $d_{\mathrm{T}} < 3\,\sigma_T$. Here σ_{T} is the quadratic sum of the uncertainty in the value of d_{T} and the root-mean-square of the beam spot distribution in the transverse plane. The agglomerative vertex-reconstruction algorithm [20] was used, with the z coordinates (and their uncertainties) of the tracks at the point of closest approach to the beam axis as input. For single-vertex events, there is no minimum requirement on the number of tracks associated with the vertex, even one-track vertices are allowed. Only tracks associated with a primary vertex are used in the analysis. If multiple vertices are present, the tracks from the highest multiplicity vertex are used. The resultant bias is negligible since the pileup rate is extremely small.

The vertex reconstruction resolution in the z direction is a strong function of the number of reconstructed tracks and it is always smaller than 0.1 cm. The distribution of the z coordinates of the reconstructed primary vertices is Gaussian, with a standard deviation of 7.1 cm. The simulated data were reweighted so as to have the same vertex z coordinate distribution as the data.

The hadron spectra were corrected for particles of non-primary origin ($\tau > 10^{-12}$ s). The main sources of secondary particles are weakly decaying particles, mostly $\mathrm{K}^0_{\mathrm{S}}$, $\Lambda/\overline{\Lambda}$, and $\Sigma^+/\overline{\Sigma}^-$. While the correction ($C_{\mathrm{s}}$) is around 1 % for pions, it rises up to 15 % for protons with $p_{\mathrm{T}} \approx 0.2\,\mathrm{GeV}/c$. As none of the mentioned weakly decaying particles decay into kaons, the correction for kaons is small. Based on studies comparing reconstructed $\mathrm{K}^0_{\mathrm{S}}$, Λ, and $\overline{\Lambda}$ spectra and predictions from the HIJING event generator, the corrections are reweighted by a p_{T}-dependent factor.

For $p < 0.15\,\mathrm{GeV}/c$, electrons can be clearly identified. The overall $\mathrm{e}^{\pm}$ contamination of the hadron yields is below 0.2 %. Although muons cannot be separated from pions, their fraction is very small, below 0.05 %. Since both contaminations are negligible, no corrections are applied for them.

3 Estimation of energy loss rate and yield extraction

In this paper an analytical parametrization [21] has been used to approximate the energy loss of charged particles in

the silicon detectors. The method provides the probability density $P(\Delta|\varepsilon, l)$ of energy deposit Δ, if the most probable energy loss rate ε at a reference path-length $l_0 = 450\,\mu\text{m}$ and the path-length l are known. It was used in conjunction with a maximum likelihood method, for the estimate of ε.

For pixel clusters, the energy deposits were calculated as the sum of individual pixel deposits. In the case of strips, the energy deposits were corrected for capacitive coupling and cross-talk between neighboring strips. The readout threshold, the coupling parameter, and the standard deviation of the Gaussian noise for strips were determined from data, using tracks with close-to-normal incidence.

For an accurate determination of ε, the response of all readout chips was calibrated with multiplicative gain correction factors. The measured energy deposit spectra were compared to the energy loss parametrization and hit-level corrections (affine transformation of energy deposits using scale factors and shifts) were introduced. The corrections were applied to individual hits during the determination of the $\ln\varepsilon$ fit templates (described below).

The best value of ε for each track was calculated with the corrected energy deposits by minimizing the joint energy deposit negative log-likelihood of all hits on the trajectory (index i), $\chi^2 = -2\sum_i \ln P(\Delta_i|\varepsilon, l_i)$. Hits with incompatible energy deposits (contributing more than 12 to the joint χ^2) were excluded. At most one hit was removed; this affected about 1.5 % of the tracks.

Distributions of $\ln\varepsilon$ as a function of total momentum p for positive particles are plotted in the top panel of Fig. 2 and compared to the predictions of the energy loss method [21] for electrons, pions, kaons, and protons. The remaining deviations were taken into account by means of track-level corrections mentioned above (affine transformation of templates using scale factors and shifts, $\ln\varepsilon \to \alpha\ln\varepsilon + \delta$).

Low-momentum particles can be identified unambiguously and can therefore be counted. Conversely, at high momentum, the $\ln\varepsilon$ bands overlap (above about 0.5 GeV/c for pions and kaons and 1.2 GeV/c for protons); the particle yields therefore need to be determined by means of a series of template fits in $\ln\varepsilon$, in bins of η and p_T (Fig. 2, bottom panel). Finally, fit templates, giving the expected $\ln\varepsilon$ distributions for all particle species (electrons, pions, kaons, and protons), were built from tracks. All kinematical parameters and hit-related observables were kept, but the energy deposits were regenerated by sampling from the analytical parametrization. For a less biased determination of track-level residual corrections, enhanced samples of each particle type were employed. These were used for setting starting values of the fits. For electrons and positrons, photon conversions in the beam-pipe and innermost first pixel layer were used. For high-purity π and enhanced p samples, weakly decaying hadrons were selected (K^0_S, $\Lambda/\overline{\Lambda}$). The relations and constraints described

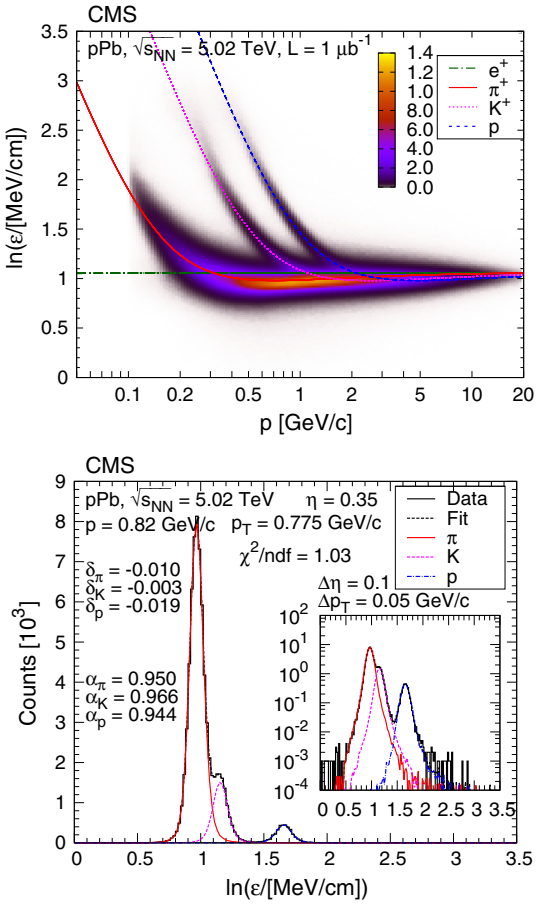

Fig. 2 *Top* distribution of $\ln\varepsilon$ as a function of total momentum p, for positively charged particles (ε is the most probable energy loss rate at a reference path length $l_0 = 450\,\mu\text{m}$). The z scale is shown in arbitrary units and is linear. The curves show the expected $\ln\varepsilon$ for electrons, pions, kaons, and protons (Eq. (30.11) in Ref. [22]). *Bottom* example $\ln\varepsilon$ distribution at $\eta = 0.35$ and $p_\text{T} = 0.775\,\text{GeV}/c$, with bin widths $\Delta\eta = 0.1$ and $\Delta p_\text{T} = 0.05\,\text{GeV}/c$. Scale factors ($\alpha$) and shifts ($\delta$) are indicated (see text). The *inset* shows the distribution with logarithmic vertical scale

in Ref. [8] were also exploited, this way better constraining the parameters of the fits: fitting the $\ln\varepsilon$ distributions in number of hits (n_hits) and track-fit χ^2/ndf slices simultaneously; fixing the distribution n_hits of particle species, relative to each other; using the expected continuity for refinement of track-level residual corrections, in neighboring (η, p_T) bins; using the expected convergence for track-level residual corrections, as the $\ln\varepsilon$ values of two particle species approach each other.

The results of the (iterative) $\ln\varepsilon$ fits are the yields for each particle species and charge in bins of (η, p_T) or (y, p_T), both inclusive and divided into classes of reconstructed primary charged-track multiplicity. In the end, the histogram fit χ^2/ndf values were usually close to unity. Although pion and kaon yields could not be determined for $p > 1.30\,\text{GeV}/c$,

their sum was measured. This information is an important constraint when fitting the p_{T} spectra.

The statistical uncertainties for the extracted yields are given by the fits. The observed local variations of parameters in the (η, p_{T}) plane for track-level corrections cannot be attributed to statistical fluctuations and indicate that the average systematic uncertainties in the scale factors and shifts are about 10^{-2} and 2×10^{-3}, respectively. These scale factors and shifts agree with those seen in the high-purity samples to well within a factor of two. The systematic uncertainties in the yields in each bin were obtained by refitting the histograms with the parameters changed by these amounts.

4 Corrections and systematic uncertainties

The measured yields in each (η, p_{T}) bin, $\Delta N_{\mathrm{measured}}$, were first corrected for the misreconstructed-track rate (C_{f}) and the fraction of secondary particles (C_{s}):

$$\Delta N' = \Delta N_{\mathrm{measured}} \cdot (1 - C_{\mathrm{f}}) \cdot (1 - C_{\mathrm{s}}). \quad (1)$$

The distributions were then unfolded to take into account the finite η and p_{T} resolutions. The η distribution of the tracks is almost flat and the η resolution is very good. Conversely, the p_{T} distribution is steep in the low-momentum region and separate corrections in each η bin were necessary. An unfolding procedure with linear regularization [23] was used, based on response matrices obtained from MC samples for each particle species.

The corrected yields were obtained by applying corrections for acceptance (C_{a}), efficiency (C_{e}), and multiple track reconstruction rate (C_{m}):

$$\frac{1}{N_{\mathrm{ev}}} \frac{\mathrm{d}^2 N}{\mathrm{d}\eta\, \mathrm{d}p_{\mathrm{T}}}_{\mathrm{corrected}} = \frac{1}{C_{\mathrm{a}} \cdot C_{\mathrm{e}} \cdot (1 + C_{\mathrm{m}})} \frac{\Delta N'}{N_{\mathrm{ev}} \Delta\eta \Delta p_{\mathrm{T}}}, \quad (2)$$

where N_{ev} is the corrected number of DS events (Fig. 1). Bins with acceptance smaller than 50 %, efficiency smaller than 50 %, multiple-track rate greater than 10 %, or containing less than 80 tracks were not used.

Finally, the differential yields $\mathrm{d}^2N/\mathrm{d}\eta\,\mathrm{d}p_{\mathrm{T}}$ were transformed to invariant yields $\mathrm{d}^2N/\mathrm{d}y\,\mathrm{d}p_{\mathrm{T}}$ by multiplying with the Jacobian E/p and the (η, p_{T}) bins were mapped into a (y, p_{T}) grid. As expected, there is a small (5–10 %) y dependence in the narrow region considered ($|y| < 1$), depending on event multiplicity. The yields as a function of p_{T} were obtained by averaging over rapidity.

The systematic uncertainties are very similar to those in Ref. [8] and are summarized in Table 1. The uncertainties of the corrections related to the event selection and pileup are fully or mostly correlated and were treated as normalization uncertainties: 3.0 % uncertainty on the yields and

Table 1 Summary of the systematic uncertainties affecting the p_{T} spectra. Values in parentheses indicate uncertainties in the $\langle p_{\mathrm{T}} \rangle$ measurement. The systematic uncertainty related to the low p_{T} extrapolation is small compared to the contributions from other sources and therefore not included in the combined systematic uncertainty of the measurement. Representative, particle-specific uncertainties (π, K, p) are given for $p_{\mathrm{T}} = 0.6\,\mathrm{GeV}/c$ in the third group of systematic uncertainties

Source	*Uncertainty of the source* [%]	*Propagated yield uncertainty* [%]		
Fully correlated, normalization				
Correction for event selection	3.0 (1.0)	4–6 (9–15)		
Pileup correction (merged and split vertices)	0.3			
High p_{T} extrapolation	2–5 (8–15)			
Mostly uncorrelated				
Pixel hit efficiency	0.3	0.3		
Misalignment, different scenarios	0.1			
Mostly uncorrelated, (y, p_{T}) dependent		π	K	p
Acceptance of the tracker	1–6	1	1	1
Efficiency of the reconstruction	3–6	3	3	3
Multiple-track reconstruction	50% of the corr.	–	–	–
Misreconstructed-track rate	50% of the corr.	0.1	0.1	0.1
Correction for secondary particles	20% of the corr.	0.2	–	2
Fitting $\ln \varepsilon$ distributions	1–10	1	2	1

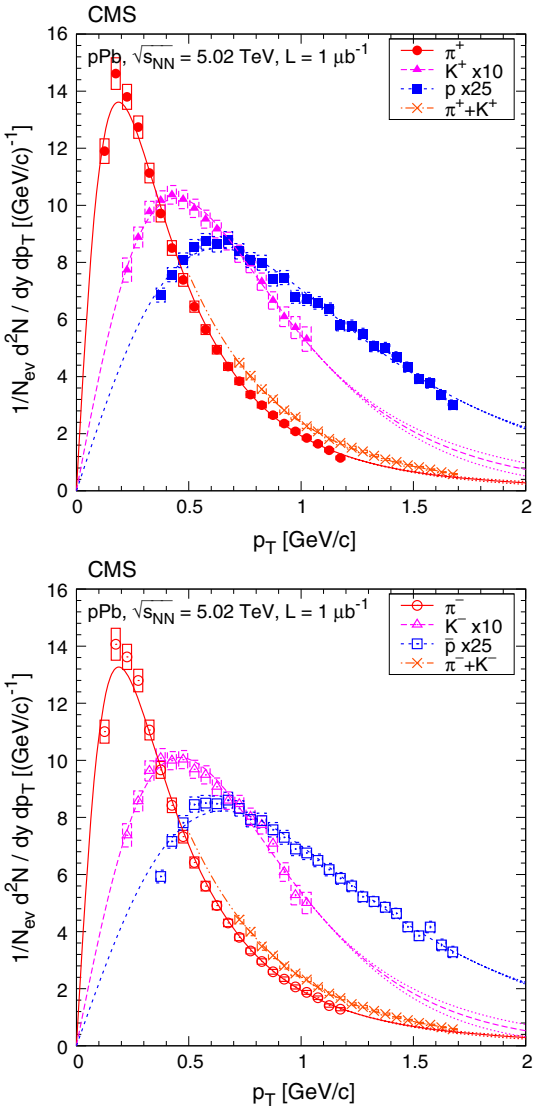

Fig. 3 Transverse momentum distributions of identified charged hadrons (pions, kaons, protons, sum of pions and kaons) in the range $|y| < 1$, for positively (*top*) and negatively (*bottom*) charged particles. Kaon and proton distributions are scaled as shown in the legends. Fits to Eqs. (3) and (5) are superimposed. *Error bars* indicate the uncorrelated statistical uncertainties, while *boxes* show the uncorrelated systematic uncertainties. The fully correlated normalization uncertainty (not shown) is 3.0 %. *Dotted lines* illustrate the effect of varying the $1/n$ value of the Tsallis–Pareto function by ±0.1 above the highest measured p_T point

1.0 % on the average p_T. In order to study the influence of the high p_T extrapolation on $\langle dN/dy \rangle$ and $\langle p_T \rangle$, the $1/n$ parameter of the fitted Tsallis–Pareto function (Sect. 5) was varied. While keeping the function in the measured range, $1/n$ was increased and decreased by ±0.1 above the highest p_T measured point, ensuring that the two function pieces are continuous both in value and derivative. The choice of the magnitude for the variation was motivated by the fitted $1/n$ values and their distance from a Boltzmann distribution. (The resulting functions are plotted in Fig. 3 as dotted lines.) The high p_T extrapolation introduces sizeable systematic uncertainties, 4–6 % for $\langle dN/dy \rangle$, and 9–15 % for $\langle p_T \rangle$ in case of the DS selection.

The tracker acceptance and the track reconstruction efficiency generally have small uncertainties (1 and 3 %, respectively), but change rapidly at very low p_T (bottom panel of Fig. 1), leading to a 6 % uncertainty on the yields in that range. For the multiple-track and misreconstructed-track rate corrections, the uncertainty is assumed to be 50 % of the correction, while for the case of the correction for secondary particles it was estimated to be 20 %. These mostly uncorrelated uncertainties are due to the imperfect modeling of the detector: regions with mismodeled efficiency in the tracker, alignment uncertainties, and channel-by-channel varying hit efficiency. These circumstances can change frequently in momentum space, so can be treated as uncorrelated.

The systematic uncertainties originating from the unfolding procedure were studied. Since the p_T response matrices are close to diagonal, the unfolding of p_T distributions did not introduce substantial systematics. At the same time the inherited uncertainties were properly propagated. The introduced correlations between neighboring p_T bins were neglected, hence statistical uncertainties were regarded as uncorrelated while systematic uncertainties were expected to be locally correlated in p_T. The systematic uncertainty of the fitted yields is in the range 1–10 % depending mostly on total momentum.

5 Results

In previously published measurements of unidentified and identified particle spectra [16,24], the following form of the Tsallis–Pareto-type distribution [25,26] was fitted to the data:

$$\frac{d^2N}{dy\, dp_T} = \frac{dN}{dy} \cdot C \cdot p_T \left[1 + \frac{m_T - m}{nT}\right]^{-n}, \tag{3}$$

where

$$C = \frac{(n-1)(n-2)}{nT[nT + (n-2)m]} \tag{4}$$

and $m_T = \sqrt{m^2 + p_T^2}$ (factors of c are omitted from the preceding formulae). The free parameters are the integrated yield dN/dy, the exponent n, and parameter T. The above formula is useful for extrapolating the spectra to zero p_T and very high p_T and for extracting $\langle p_T \rangle$ and dN/dy. Its validity for different multiplicity bins was cross-checked by fitting MC spectra in the p_T ranges where there are data points, and verifying that the fitted values of $\langle p_T \rangle$ and dN/dy were consistent with the generated values. Nevertheless, for a more robust estimation of both quantities ($\langle p_T \rangle$ and $\langle dN/dy \rangle$), the data points and their uncertainties were used in the measured

range and the fitted functions only for the extrapolation in the unmeasured regions. According to some models of particle production based on non-extensive thermodynamics [26], the parameter T is connected with the average particle energy, while n characterizes the "non-extensivity" of the process, i.e. the departure of the spectra from a Boltzmann distribution ($n = \infty$).

As discussed earlier, pions and kaons cannot be unambiguously distinguished at higher momenta. Because of this, the pion-only, the kaon-only, and the joint pion and kaon $\mathrm{d}^2N/\mathrm{d}y\,\mathrm{d}p_\mathrm{T}$ distributions were fitted for $|y| < 1$ and $p < 1.20\,\mathrm{GeV}/c$, $|y| < 1$ and $p < 1.05\,\mathrm{GeV}/c$, and $|\eta| < 1$ and $1.05 < p < 1.7\,\mathrm{GeV}/c$, respectively. Since the ratio p/E for the pions (which are more abundant than kaons) at these momenta can be approximated by $p_\mathrm{T}/m_\mathrm{T}$ at $\eta \approx 0$, Eq. (3) becomes:

$$\frac{\mathrm{d}^2N}{\mathrm{d}\eta\,\mathrm{d}p_\mathrm{T}} \approx \frac{\mathrm{d}N}{\mathrm{d}y} \cdot C \cdot \frac{p_\mathrm{T}^2}{m_\mathrm{T}} \left(1 + \frac{m_\mathrm{T} - m}{nT}\right)^{-n}. \tag{5}$$

The approximate fractions of particles outside the measured p_T range depend on track multiplicity; they are 15–30 % for pions, 40–50 % for kaons, and 20–35 % for protons. The average transverse momentum $\langle p_\mathrm{T}\rangle$ and its uncertainty were obtained using data points in the measured range complemented by numerical integration of Eq. (3) with the fitted parameters in the unmeasured regions, under the assumption that the particle yield distributions follow the Tsallis–Pareto function in the low-p_T and high-p_T regions.

The results discussed in the following are for laboratory rapidity $|y| < 1$. In all cases, error bars indicate the uncorrelated statistical uncertainties, while boxes show the uncorrelated systematic uncertainties. The fully correlated normalization uncertainty is not shown. For the p_T spectra, the average transverse momentum, and the ratio of particle yields, the data are compared to AMPT 1.26/2.26 [13], EPOS LHC [14,15], and HIJING 2.1 [11] MC event generators. Numerical results corresponding to the plotted spectra, fit results, as well as their statistical and systematic uncertainties are given in Ref. [27].

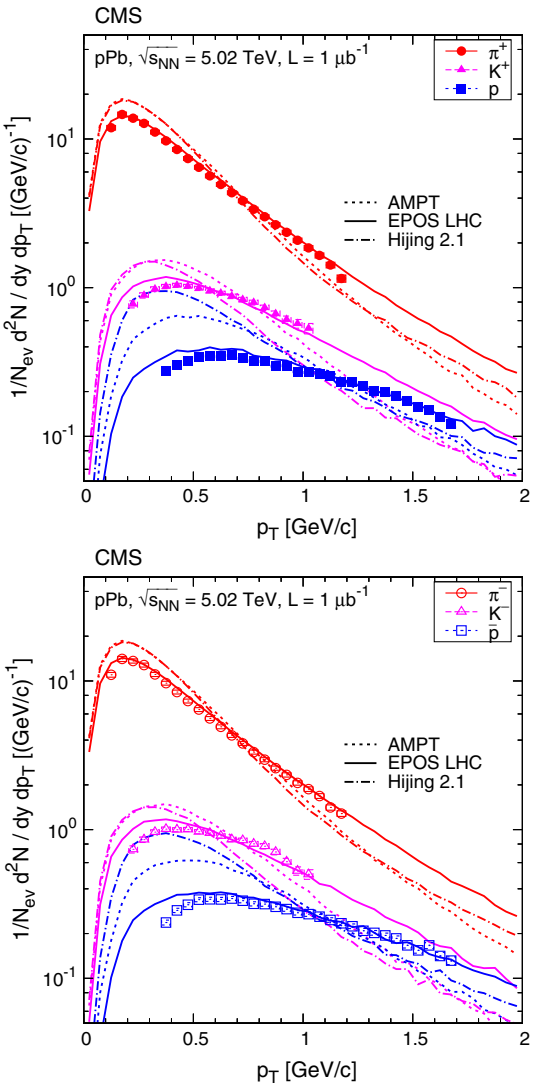

Fig. 4 Transverse momentum distributions of identified charged hadrons (pions, kaons, protons) in the range $|y| < 1$, for positively (*top*) and negatively (*bottom*) charged particles. Measured values (same as in Fig. 3) are plotted together with predictions from AMPT, EPOS LHC, and HIJING. *Error bars* indicate the uncorrelated statistical uncertainties, while *boxes* show the uncorrelated systematic uncertainties. The fully correlated normalization uncertainty (not shown) is 3.0 %

Table 2 Fit results ($\mathrm{d}N/\mathrm{d}y$, $1/n$, and T) and goodness-of-fit values for the DS selection shown together with calculated averages ($\langle \mathrm{d}N/\mathrm{d}y\rangle$, $\langle p_\mathrm{T}\rangle$) for charged pions, kaons, and protons. The systematic uncertainty related to the low p_T extrapolation is small compared to the contributions from other sources and therefore not included in the combined systematic uncertainty of the measurement. Combined uncertainties are given

Particle	$\mathrm{d}N/\mathrm{d}y$	$1/n$	T (GeV/c)	χ^2/ndf	$\langle \mathrm{d}N/\mathrm{d}y\rangle$	$\langle p_\mathrm{T}\rangle$ (GeV/c)
π^+	8.074 ± 0.081	0.190 ± 0.007	0.131 ± 0.003	0.88	8.064 ± 0.190	0.547 ± 0.078
π^-	7.971 ± 0.079	0.195 ± 0.007	0.131 ± 0.003	1.05	7.966 ± 0.196	0.559 ± 0.083
K^+	1.071 ± 0.068	0.092 ± 0.066	0.278 ± 0.022	0.42	1.040 ± 0.053	0.790 ± 0.104
K^-	0.984 ± 0.047	-0.008 ± 0.067	0.316 ± 0.024	2.82	0.990 ± 0.037	0.744 ± 0.061
p	0.510 ± 0.018	0.151 ± 0.036	0.325 ± 0.016	0.81	0.510 ± 0.024	1.243 ± 0.183
$\bar{\mathrm{p}}$	0.494 ± 0.017	0.123 ± 0.038	0.349 ± 0.017	1.32	0.495 ± 0.022	1.215 ± 0.165

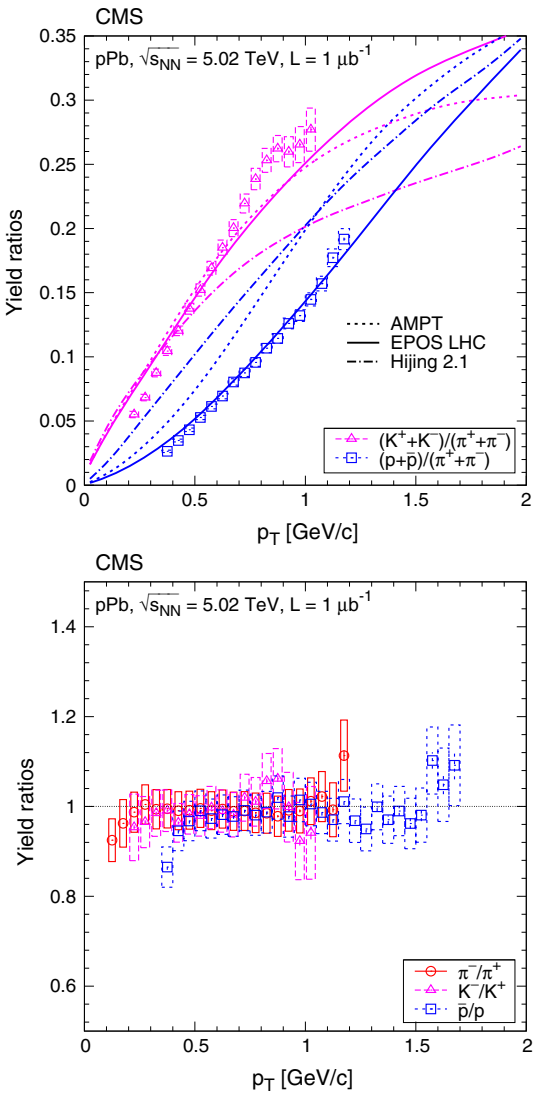

Fig. 5 Ratios of particle yields as a function of transverse momentum. K/π and p/π values are shown in the *top* panel, and opposite-charge ratios are plotted in the *bottom* panel. *Error bars* indicate the uncorrelated statistical uncertainties, while *boxes* show the uncorrelated systematic uncertainties. In the *top* panel, *curves* indicate predictions from AMPT, EPOS LHC, and HIJING

5.1 Inclusive measurements

The transverse momentum distributions of positively and negatively charged hadrons (pions, kaons, protons) are shown in Fig. 3, along with the results of the fits to the Tsallis–Pareto parametrization (Eqs. (3) and (5)). The fits are of good quality with χ^2/ndf values in the range 0.4–2.8 (Table 2). Figure 4 presents the data compared to the AMPT, EPOS LHC, and HIJING predictions. EPOS LHC gives a good description, while other generators predict steeper p_T distributions than found in data.

Ratios of particle yields as a function of the transverse momentum are plotted in Fig. 5. While the K/π ratios are

Table 3 Relationship between the number of reconstructed tracks (N_{rec}) and the average number of corrected tracks ($\langle N_{tracks} \rangle$) in the region $|\eta| < 2.4$, and also with the condition $p_T > 0.4$ GeV/c (used in Ref. [29]), in the 19 multiplicity classes considered

N_{rec}	0–9	10–19	20–29	30–39	40–49	50–59	60–69	70–79	80–89	90–99	100–109	110–119	120–129	130–139	140–149	150–159	160–169	170–179	180–189
$\langle N_{tracks} \rangle$	8	19	32	45	58	71	84	96	109	122	135	147	160	173	185	198	210	222	235
$\langle N_{tracks} \rangle_{p_T>0.4\,GeV/c}$	3	8	15	22	29	36	43	50	58	65	73	80	87	95	103	110	117	125	133

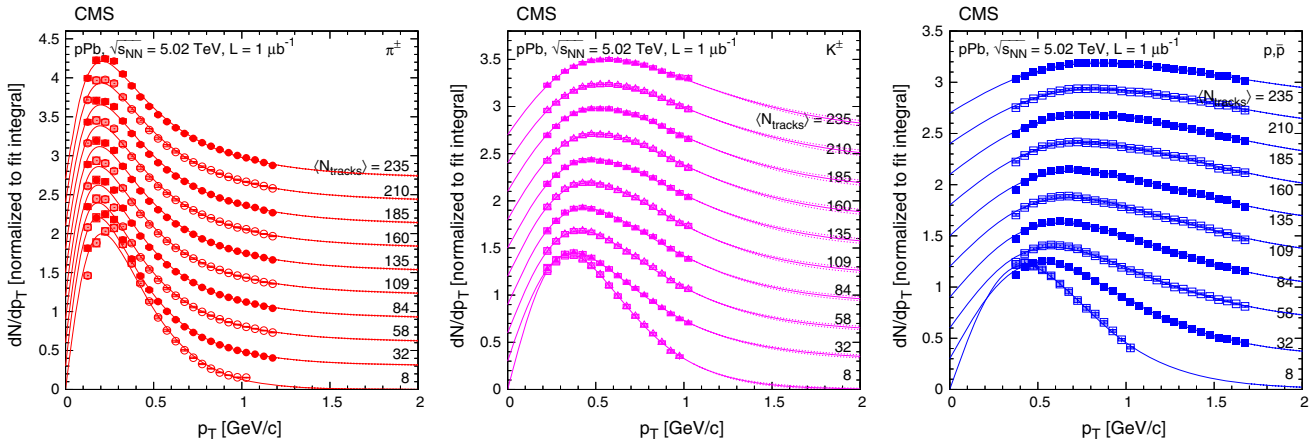

Fig. 6 Transverse momentum distributions of charged pions, kaons, and protons, normalized such that the fit integral is unity, in every second multiplicity class ($\langle N_{\text{tracks}} \rangle$ values are indicated) in the range $|y| < 1$, fitted with the Tsallis–Pareto parametrization (*solid lines*). For better visibility, the result for any given $\langle N_{\text{tracks}} \rangle$ bin is shifted by 0.3 units with respect to the adjacent bins. *Error bars* indicate the uncorrelated statistical uncertainties, while *boxes* show the uncorrelated systematic uncertainties. *Dotted lines* illustrate the effect of varying the $1/n$ value of the Tsallis–Pareto function by ± 0.1 above the highest measured p_{T} point

well described by the AMPT simulation, only EPOS LHC is able to predict both K/π and p/π ratios. The ratios of the yields for oppositely charged particles are close to one, as expected for LHC energies at midrapidity.

5.2 Multiplicity dependent measurements

A study of the dependence on track multiplicity is motivated partly by the intriguing hadron correlations measured in pp and pPb collisions at high track multiplicities [28–31], suggesting possible collective effects in "central" pp and pPb collisions at the LHC. At the same time, it was seen that in pp collisions the characteristics of particle production ($\langle p_{\text{T}} \rangle$, ratios) at LHC energies are strongly correlated with event particle multiplicity rather than with the center-of-mass energy of the collision [8]. The strong dependence on multiplicity (or centrality) was also seen in dAu collisions at RHIC [6,7]. In addition, the multiplicity dependence of particle yield ratios is sensitive to various final-state effects (hadronization, color reconnection, collective flow) implemented in MC models used in collider and cosmic-ray physics [32].

The event multiplicity N_{rec} is obtained from the number of reconstructed tracks with $|\eta| < 2.4$, where the tracks are reconstructed using the same algorithm as for the identified charged hadrons [18]. (The multiplicity variable $N_{\text{trk}}^{\text{offline}}$, used in Ref. [29], is obtained from a different track reconstruction configuration and a value of $N_{\text{trk}}^{\text{offline}} = 110$ corresponds roughly to $N_{\text{rec}} = 170$.) The event multiplicity was divided into 19 classes, defined in Table 3. To facilitate comparisons with models, the corresponding corrected charged particle multiplicity in the same acceptance of $|\eta| < 2.4$ (N_{tracks}) is also determined. For each multiplicity class, the correction from N_{rec} to N_{tracks} uses the efficiency estimated with the HIJING simulation in (η, p_{T}) bins. The corrected data are then integrated over p_{T}, down to zero yield at $p_{\text{T}} = 0$ (with a linear extrapolation below $p_{\text{T}} = 0.1$ GeV/c). Finally, the integrals for each eta slice are summed. The average corrected charged-particle multiplicity $\langle N_{\text{tracks}} \rangle$, and also its values with the condition $p_{\text{T}} > 0.4$ GeV/c, are shown in Table 3 for each event multiplicity class. The value of $\langle N_{\text{tracks}} \rangle$ is used to identify the multiplicity class in Figs. 6, 7, 8, 9, and 10.

Transverse-momentum distributions of identified charged hadrons, normalized such that the fit integral is unity, in selected multiplicity classes for $|y| < 1$ are shown in Fig. 6 for pions, kaons, and protons. The distributions of negatively and positively charged particles have been summed. The distributions are fitted with the Tsallis–Pareto parametrization with χ^2/ndf values in the range 0.8–4.0 for pions, 0.1–1.1 for kaons, and 0.1–0.7 for protons. For kaons and protons, the parameter T increases with multiplicity, while for pions T slightly increases and the exponent n slightly decreases with multiplicity (not shown).

The ratios of particle yields are displayed as a function of track multiplicity in Fig. 7. The K/π and p/π ratios are flat, or slightly rising, as a function of $\langle N_{\text{tracks}} \rangle$. While none of the models is able to precisely reproduce the track multiplicity dependence, the best and worst matches to the overall scale are given by EPOS LHC and HIJING, respectively. The ratios of yields of oppositely charged particles are independent of $\langle N_{\text{tracks}} \rangle$ as shown in the bottom panel of Fig. 7. The average transverse momentum $\langle p_{\text{T}} \rangle$ is shown as a function of multiplicity in Fig. 8. As expected from the discrepancies between theory and data shown in Fig. 4, EPOS LHC again gives a reasonable description, while the other event generators presented here underpredict the measured values. For the dependence of T on multiplicity (not shown), the predic-

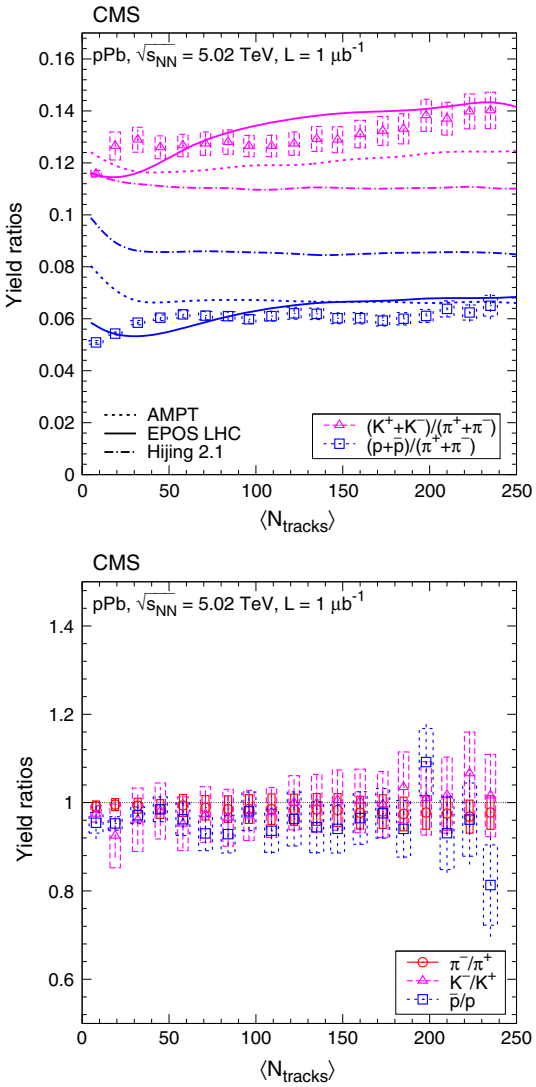

Fig. 7 Ratios of particle yields in the range $|y| < 1$ as a function of the corrected track multiplicity for $|\eta| < 2.4$. K/π and p/π values are shown in the *top* panel, and opposite-charge ratios are plotted in the *bottom* panel. *Error bars* indicate the uncorrelated combined uncertainties, while *boxes* show the uncorrelated systematic uncertainties. In the *top* panel, curves indicate predictions from AMPT, EPOS LHC, and HIJING

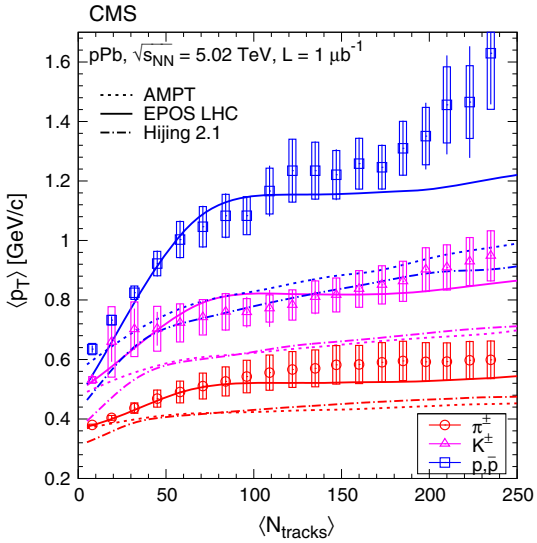

Fig. 8 Average transverse momentum of identified charged hadrons (pions, kaons, protons) in the range $|y| < 1$, as a function of the corrected track multiplicity for $|\eta| < 2.4$, computed assuming a Tsallis–Pareto distribution in the unmeasured range. *Error bars* indicate the uncorrelated combined uncertainties, while boxes show the uncorrelated systematic uncertainties. The fully correlated normalization uncertainty (not shown) is 1.0 %. *Curves* indicate predictions from AMPT, EPOS LHC, and HIJING

tions match the pion data well; the kaon and proton values are much higher than in AMPT or HIJING.

5.3 Comparisons to pp and PbPb data

The comparison with pp data taken at various center-of-mass energies (0.9, 2.76, and 7 TeV) [8] is shown in Fig. 9, where the dependence of $\langle p_T \rangle$ and the particle yield ratios (K/π and p/π) on the track multiplicity is shown. The plots also display the ranges of these values measured by ALICE in PbPb collisions at $\sqrt{s_{NN}} = 2.76$ TeV for centralities from peripheral (80–90 % of the inelastic cross-section) to central (0–5 %) [33]. These ALICE PbPb data cover a much wider range of N_{tracks} than is shown in the plot. Although PbPb data are not available at $\sqrt{s_{NN}} = 5.02$ TeV for comparison, the evolution of event characteristics from RHIC ($\sqrt{s_{NN}} = 0.2$ TeV, [3,4,6]) to LHC energies [33] suggests that yield ratios should remain similar, while $\langle p_T \rangle$ values will increase by about 5 % when going from $\sqrt{s_{NN}} = 2.76$ TeV to 5.02 TeV.

For low track multiplicity ($N_{tracks} \lesssim 40$), pPb collisions behave very similarly to pp collisions, while at higher multiplicities ($N_{tracks} \gtrsim 50$) the $\langle p_T \rangle$ is lower for pPb than in pp. The first observation can be explained since low-multiplicity events are peripheral pPb collisions in which only a few proton–nucleon collisions are present. Events with more particles are indicative of collisions in which the projectile proton strikes the thick disk of the lead nucleus. Interestingly, the pPb curves (Fig. 9, top panel) can be reasonably approximated by taking the pp values and multiplying their N_{tracks} coordinate by a factor of 1.8, for all particle types. In other words, a pPb collision with a given N_{tracks} is similar to a pp collision with $0.55 \times N_{tracks}$ for produced charged particles in the $|\eta| < 2.4$ range. Both the highest-multiplicity pp and pPb interactions yield higher $\langle p_T \rangle$ than seen in central PbPb collisions. While in the PbPb case even the most central collisions possibly contain a mix of soft (lower-$\langle p_T \rangle$) and hard (higher-$\langle p_T \rangle$) nucleon-nucleon interactions, for pp or pPb collisions the most violent interaction or sequence of interactions are selected.

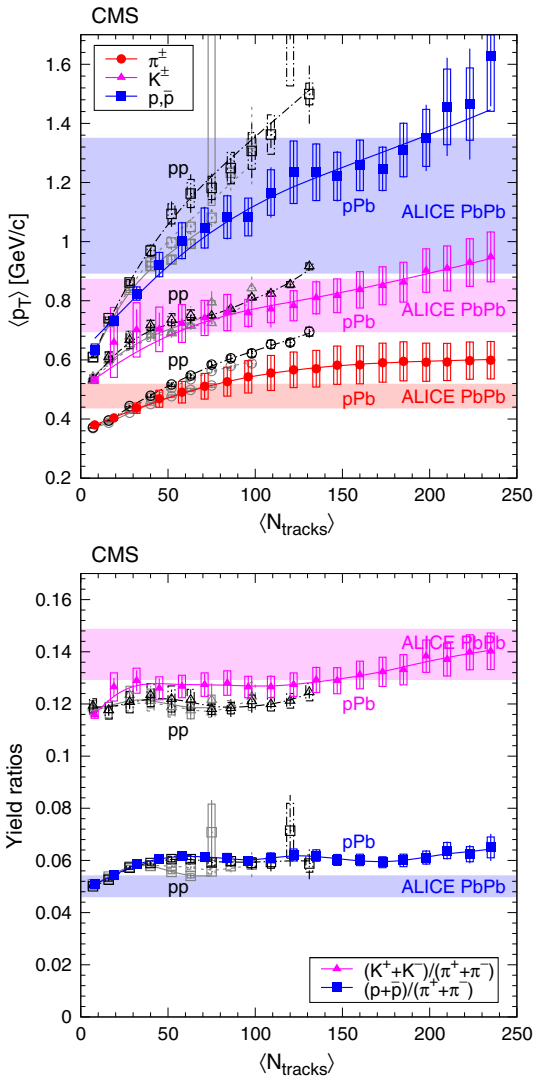

Fig. 9 Average transverse momentum of identified charged hadrons (pions, kaons, protons; *top* panel) and ratios of particle yields (*bottom* panel) in the range $|y| < 1$ as a function of the corrected track multiplicity for $|\eta| < 2.4$, for pp collisions (*open symbols*) at several energies [8], and for pPb collisions (*filled symbols*) at $\sqrt{s_{NN}} = 5.02$ TeV. Both $\langle p_T \rangle$ and yield ratios were computed assuming a Tsallis–Pareto distribution in the unmeasured range. *Error bars* indicate the uncorrelated combined uncertainties, while *boxes* show the uncorrelated systematic uncertainties. For $\langle p_T \rangle$ the fully correlated normalization uncertainty (not shown) is 1.0 %. In both plots, lines are drawn to guide the eye (*gray solid* pp 0.9 TeV, *gray dotted* pp 2.76 TeV, *black dash-dotted* pp 7 TeV, *colored solid* pPb 5.02 TeV). The ranges of $\langle p_T \rangle$, K/π and p/π values measured by ALICE in various centrality PbPb collisions (see text) at $\sqrt{s_{NN}} = 2.76$ TeV [33] are indicated with *horizontal bands*

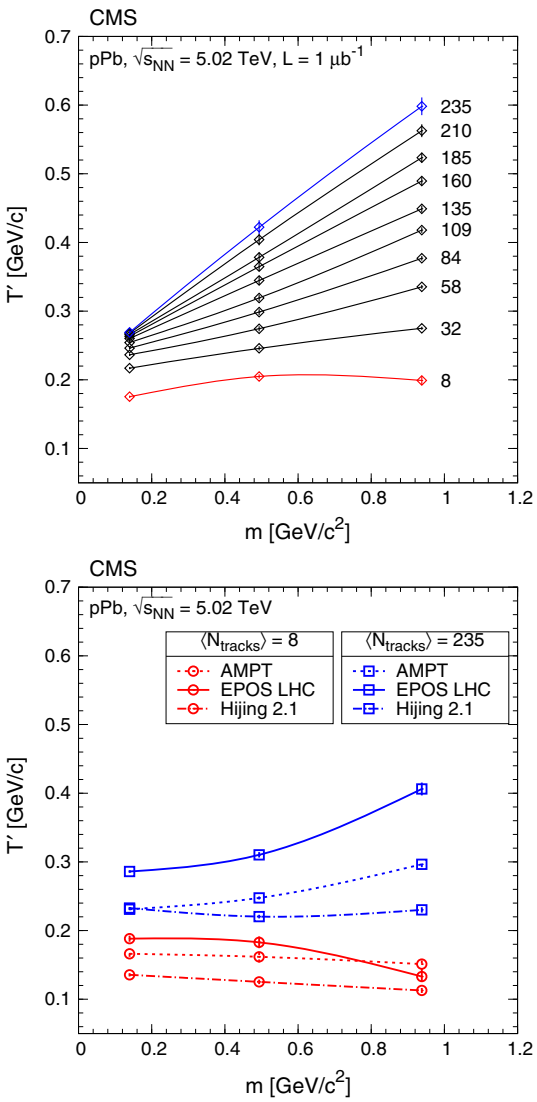

Fig. 10 Inverse slope parameters T' from fits of pion, kaon, and proton spectra (both charges) with a form proportional to $p_T \exp(-m_T/T')$. Results for a selection of multiplicity classes, with different $\langle N_{tracks} \rangle$ as indicated, are plotted for pPb data (*top*) and for MC event generators AMPT, EPOS LHC, and HIJING (*bottom*). The *curves* are drawn to guide the eye

The transverse momentum spectra could also be successfully fitted (χ^2/ndf in the range 0.7–1.8) with a functional form proportional to $p_T \exp(-m_T/T')$, where T' is called the inverse slope parameter, motivated by the success of Boltzmann-type distributions in nucleus–nucleus collisions [34]. In the case of pions, the fitted range was restricted to $m_T > 0.4$ GeV/c in order to exclude the region where resonance decays would significantly contribute to the measured spectra. The inverse slope parameter as a function of hadron mass is shown in Fig. 10, for a selection of event classes, both for pPb data and for MC event generators (AMPT, EPOS LHC, and HIJING). While the data display a linear dependence on mass with a slope that increases with particle multiplicity, the models predict a flat or slowly rising behavior versus mass and only limited changes with track multiplicity. This is to be compared with pp results [8], where both data and several tunes of the PYTHIA 6 [35] and PYTHIA 8 event generators show features very similar to those in pPb data. A similar trend is also observed in nucleus–nucleus collisions [3,6],

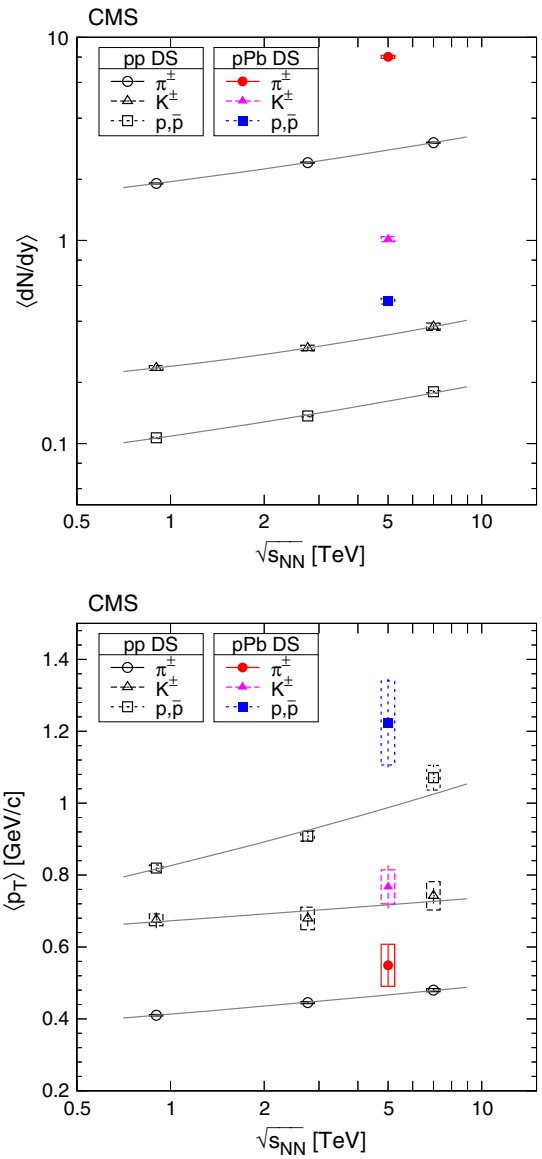

Fig. 11 Average rapidity densities $\langle dN/dy \rangle$ (*top*) and average transverse momenta $\langle p_T \rangle$ (*bottom*) as a function of center-of-mass energy for pp [8] and pPb collisions, for charge-averaged pions, kaons, and protons. *Error bars* indicate the uncorrelated combined uncertainties, while *boxes* show the uncorrelated systematic uncertainties. The *curves* show parabolic (for $\langle dN/dy \rangle$) or linear (for $\langle p_T \rangle$) interpolation on a log-log scale. The pp and pPb data are for laboratory rapidity $|y| < 1$, which is the same as the center-of-mass rapidity only for the pp data

which is attributed to the effect of radial flow velocity boost [1].

Average rapidity densities $\langle dN/dy \rangle$ and average transverse momenta $\langle p_T \rangle$ of charge-averaged pions, kaons, and protons as a function of center-of-mass energy are shown in Fig. 11 for pp and pPb collisions, both corrected to the DS selection. To allow comparison at the pPb energy, a parabolic (linear) interpolation of the pp collision values at $\sqrt{s} = 0.9$, 2.76, and 7 TeV is shown for dN/dy ($\langle p_T \rangle$). The rapidity densities are generally about three times greater than in pp interactions at the same energy, while the average transverse momentum increases by about 20, 10, and 30 % for pions, kaons, and protons, respectively. The factor of three difference in the yields for pPb as compared to pp can be compared with the estimated number of projectile collisions $N_{\text{coll}}/2 = 3.5 \pm 0.3$ or with the number of nucleons participating in the collision $N_{\text{part}}/2 = 4.0 \pm 0.3$, based on the ratio of preliminary pPb and pp cross-section measurements, that have proven to be good scaling variables in proton–nucleus collisions at lower energies [36].

6 Conclusions

Measurements of identified charged hadron spectra produced in pPb collisions at $\sqrt{s_{NN}} = 5.02$ TeV have been presented, normalized to events with simultaneous hadronic activity at pseudorapidities $-5 < \eta < -3$ and $3 < \eta < 5$. Charged pions, kaons, and protons were identified from the energy deposited in the silicon tracker and other track information. In the present analysis, the yield and spectra of identified hadrons for laboratory rapidity $|y| < 1$ have been studied as a function of the event charged particle multiplicity in the range $|\eta| < 2.4$. The p_T spectra are well described by fits with the Tsallis–Pareto parametrization. The ratios of the yields of oppositely charged particles are close to one, as expected at mid-rapidity for collisions of this energy. The average p_T is found to increase with particle mass and the event multiplicity. These results are valid under the assumption that the particle yield distributions follow the Tsallis–Pareto function in the unmeasured p_T regions.

The results can be used to further constrain models of hadron production and contribute to the understanding of basic non-perturbative dynamics in hadron collisions. The EPOS LHC event generator reproduces several features of the measured distributions, a significant improvement from the previous version, attributed to a new viscous hydrodynamic treatment of the produced particles. Other studied generators (AMPT, HIJING) predict steeper p_T distributions and much smaller $\langle p_T \rangle$ than found in data, as well as substantial deviations in the p/π ratios.

Combined with similar results from pp collisions, the track multiplicity dependence of the average transverse momentum and particle ratios indicate that particle production at LHC energies is strongly correlated with event particle multiplicity in both pp and pPb interactions. For low track multiplicity, pPb collisions appear similar to pp collisions. At high multiplicities, the average p_T of particles from pPb collisions with a charged particle multiplicity of N_{tracks} (in $|\eta| < 2.4$) is similar to that for pp collisions with $0.55 \times N_{\text{tracks}}$. Both the highest-multiplicity pp and pPb interactions yield higher $\langle p_T \rangle$ than seen in central PbPb collisions.

Acknowledgments We congratulate our colleagues in the CERN accelerator departments for the excellent performance of the LHC and thank the technical and administrative staffs at CERN and at other CMS institutes for their contributions to the success of the CMS effort. In addition, we gratefully acknowledge the computing centres and personnel of the Worldwide LHC Computing Grid for delivering so effectively the computing infrastructure essential to our analyses. Finally, we acknowledge the enduring support for the construction and operation of the LHC and the CMS detector provided by the following funding agencies: the Austrian Federal Ministry of Science and Research and the Austrian Science Fund; the Belgian Fonds de la Recherche Scientifique, and Fonds voor Wetenschappelijk Onderzoek; the Brazilian Funding Agencies (CNPq, CAPES, FAPERJ, and FAPESP); the Bulgarian Ministry of Education, Youth and Science; CERN; the Chinese Academy of Sciences, Ministry of Science and Technology, and National Natural Science Foundation of China; the Colombian Funding Agency (COLCIENCIAS); the Croatian Ministry of Science, Education and Sport; the Research Promotion Foundation, Cyprus; the Ministry of Education and Research, Recurrent financing contract SF0690030s09 and European Regional Development Fund, Estonia; the Academy of Finland, Finnish Ministry of Education and Culture, and Helsinki Institute of Physics; the Institut National de Physique Nucléaire et de Physique des Particules/CNRS, and Commissariat à l'Énergie Atomique et aux Énergies Alternatives/CEA, France; the Bundesministerium für Bildung und Forschung, Deutsche Forschungsgemeinschaft, and Helmholtz-Gemeinschaft Deutscher Forschungszentren, Germany; the General Secretariat for Research and Technology, Greece; the National Scientific Research Foundation, and National Office for Research and Technology, Hungary; the Department of Atomic Energy and the Department of Science and Technology, India; the Institute for Studies in Theoretical Physics and Mathematics, Iran; the Science Foundation, Ireland; the Istituto Nazionale di Fisica Nucleare, Italy; the Korean Ministry of Education, Science and Technology and the World Class University program of NRF, Republic of Korea; the Lithuanian Academy of Sciences; the Mexican Funding Agencies (CINVESTAV, CONACYT, SEP, and UASLP-FAI); the Ministry of Science and Innovation, New Zealand; the Pakistan Atomic Energy Commission; the Ministry of Science and Higher Education and the National Science Centre, Poland; the Fundaç ao para a Ciência e a Tecnologia, Portugal; JINR (Armenia, Belarus, Georgia, Ukraine, Uzbekistan); the Ministry of Education and Science of the Russian Federation, the Federal Agency of Atomic Energy of the Russian Federation, Russian Academy of Sciences, and the Russian Foundation for Basic Research; the Ministry of Science and Technological Development of Serbia; the Secretaría de Estado de Investigación, Desarrollo e Innovación and Programa Consolider-Ingenio 2010, Spain; the Swiss Funding Agencies (ETH Board, ETH Zurich, PSI, SNF, UniZH, Canton Zurich, and SER); the National Science Council, Taipei; the Thailand Center of Excellence in Physics, the Institute for the Promotion of Teaching Science and Technology of Thailand and the National Science and Technology Development Agency of Thailand; the Scientific and Technical Research Council of Turkey, and Turkish Atomic Energy Authority; the Science and Technology Facilities Council, UK; the US Department of Energy, and the US National Science Foundation. Individuals have received support from the Marie-Curie programme and the European Research Council and EPLANET (European Union); the Leventis Foundation; the A. P. Sloan Foundation; the Alexander von Humboldt Foundation; the Belgian Federal Science Policy Office; the Fonds pour la Formation à la Recherche dans l'Industrie et dans l'Agriculture (FRIA-Belgium); the Agentschap voor Innovatie door Wetenschap en Technologie (IWT-Belgium); the Ministry of Education, Youth and Sports (MEYS) of Czech Republic; the Council of Science and Industrial Research, India; the Compagnia di San Paolo (Torino); the HOMING PLUS programme of Foundation for Polish Science, cofinanced by EU, Regional Development Fund; and the Thalis and Aristeia programmes cofinanced by EU-ESF and the Greek NSRF.

References

1. E. Schnedermann, J. Sollfrank, U.W. Heinz, Thermal phenomenology of hadrons from 200 A GeV S+S collisions. Phys. Rev. C **48**, 2462 (1993). doi:10.1103/PhysRevC.48.2462. arXiv:nucl-th/9307020
2. P. Huovinen, P.V. Ruuskanen, Hydrodynamic models for heavy ion collisions. Annu. Rev. Nucl. Part. Sci. **56**, 163 (2006). doi:10.1146/annurev.nucl.54.070103.181236. arXiv:nucl-th/0605008
3. PHENIX Collaboration, Identified charged particle spectra and yields in Au+Au collisions at $\sqrt{s_{NN}}$ = 200 GeV. Phys. Rev. C **69**, 034909 (2004). doi:10.1103/PhysRevC.69.034909. arXiv:nucl-ex/0307022
4. BRAHMS Collaboration, Centrality dependent particle production at $y = 0$ and $y \sim 1$ in Au+Au collisions at $\sqrt{s_{NN}} = 200$ GeV. Phys. Rev. C **72**, 014908 (2005). doi:10.1103/PhysRevC.72.014908. arXiv:nucl-ex/0503010
5. PHOBOS Collaboration, Identified hadron transverse momentum spectra in Au+Au collisions at $\sqrt{s_{NN}} = 62.4$ GeV. Phys. Rev. C **75**, 024910 (2007). doi:10.1103/PhysRevC.75.024910. arXiv:nucl-ex/0610001
6. S.T.A.R. Collaboration, Systematic measurements of identified particle spectra in pp, d+Au and Au+Au collisions at the star detector. Phys. Rev. C **79**, 034909 (2009). doi:10.1103/PhysRevC.79.034909. arXiv:0808.2041
7. PHENIX Collaboration, Spectra and ratios of identified particles in Au+Au and d +Au collisions at $\sqrt{s_{NN}}$ = 200 GeV. Phys. Rev. C. (2013). arXiv:1304.3410
8. C.M.S. Collaboration, Study of the inclusive production of charged pions, kaons, and protons in pp collisions at $\sqrt{s}$ = 0.9, 2.76, and 7 tev. Eur. Phys. J. C **72**, 2164 (2012). doi:10.1140/epjc/s10052-012-2164-1. arXiv:1207.4724
9. ALICE Collaboration, Multiplicity dependence of pion, kaon, proton and lambda production in p-Pb collisions at $\sqrt{s_{NN}}$ = 5.02 TeV. Phys. Lett. B (2013). doi:10.1016/j.physletb.2013.11.020. arXiv:1307.6796
10. C.M.S. Collaboration, The cms experiment at the cern lhc. JINST **3**, S08004 (2008). doi:10.1088/1748-0221/3/08/S08004
11. W.-T. Deng, X.-N. Wang, R. Xu, Hadron production in p+p, p+Pb, and Pb+Pb collisions with the hijing 2.0 model at energies available at the cern large hadron collider. Phys. Rev. C **83**, 014915 (2011). doi:10.1103/PhysRevC.83.014915. arXiv:1008.1841
12. R. Xu, W.-T. Deng, X.-N. Wang, Nuclear modification of high-p_{T} hadron spectra in p+A collisions at LHC. Phys. Rev. C **86**, 051901 (2012). doi:10.1103/PhysRevC.86.051901. arXiv:1204.1998
13. Z.W. Lin, Current status and further improvements of a multi-phase transport (ampt) model. Indian J. Phys. **85**, 837 (2011). doi:10.1007/s12648-011-0086-7
14. K. Werner, F.-M. Liu, T. Pierog, Parton ladder splitting and the rapidity dependence of transverse momentum spectra in deuteron-gold collisions at rhic. Phys. Rev. C **74**, 044902 (2006). doi:10.1103/PhysRevC.74.044902. arXiv:hep-ph/0506232
15. T. Pierog et al., EPOS LHC: test of collective hadronization with LHC data (2013). arXiv:1306.0121
16. CMS Collaboration, Transverse momentum and pseudorapidity distributions of charged hadrons in pp collisions at $\sqrt{s}$ = 0.9 and 2.36 TeV. JHEP **02**, 041 (2010). doi:10.1007/JHEP02(2010)041, arXiv:1002.0621

17. S. Agostinelli et al., Geant4—a simulation toolkit. Nucl. Instrum. Methods A **506**, 250 (2003). doi:10.1016/S0168-9002(03)01368-8
18. F. Siklér, Low p_T hadronic physics with CMS. Int. J. Mod. Phys. E **16**, 1819 (2007). doi:10.1142/S0218301307007052. arXiv:physics/0702193
19. C.M.S. Collaboration, Transverse-momentum and pseudorapidity distributions of charged hadrons in pp collisions at $\sqrt{s} = 7$ tev. Phys. Rev. Lett. **105**, 022002 (2010). doi:10.1103/PhysRevLett.105.022002. arXiv:1005.3299
20. F. Siklér, Study of clustering methods to improve primary vertex finding for collider detectors. Nucl. Instrum. Methods A **621**, 526 (2010). doi:10.1016/j.nima.2010.04.058. arXiv:0911.2767
21. F. Siklér, A parametrisation of the energy loss distributions of charged particles and its applications for silicon detectors. Nucl. Instrum. Methods A **691**, 16 (2012). doi:10.1016/j.nima.2012.06.064. arXiv:1111.3213
22. Particle Data Group, J. Beringer et al., Review of particle physics.Phys. Rev. D **86**, 010001 (2012). doi:10.1103/PhysRevD.86.010001
23. W.H. Press, B.P. Flannery, S.A. Teukolsky, W.T. Vetterling, *Numerical Recipes: The Art of Scientific Computing*, 3rd edn. (Cambridge University Press, Cambridge, 2007)
24. CMS Collaboration, Strange particle production in pp collisions at $\sqrt{s}$ = 0.9 and 7 TeV. JHEP **05**, 064 (2011). doi:10.1007/JHEP05(2011)064. arXiv:1102.4282
25. C. Tsallis, Possible generalization of Boltzmann–Gibbs statistics. J. Stat. Phys. **52**, 479 (1988). doi:10.1007/BF01016429
26. T.S. Biró, G. Purcsel, K. Ürmössy, Non-extensive approach to quark matter. Eur. Phys. J. A **40**, 325 (2009). doi:10.1140/epja/i2009-10806-6. arXiv:0812.2104
27. https://twiki.cern.ch/twiki/bin/view/CMSPublic/PhysicsResultsHIN12016#Data (2014)
28. C.M.S. Collaboration, Observation of long-range near-side angular correlations in proton–proton collisions at the LHC. JHEP **09**, 091 (2010). doi:10.1007/JHEP09(2010)091. arXiv:1009.4122
29. C.M.S. Collaboration, Observation of long-range near-side angular correlations in proton-lead collisions at the LHC. Phys. Lett. B **718**, 795 (2013). doi:10.1016/j.physletb.2012.11.025. arXiv:1210.5482
30. ALICE Collaboration, Long-range angular correlations on the near and away side in p-Pb collisions at $\sqrt{s_{NN}} = 5.02$ TeV. Phys. Lett. B **719**, 29 (2013). doi:10.1016/j.physletb.2013.01.012. arXiv:1212.2001
31. ATLAS Collaboration, Observation of associated near-side and away-side long-range correlations in $\sqrt{s_{NN}}$=5.02 TeV proton-lead collisions with the ATLAS detector. Phys. Rev. Lett. **110**, 182302 (2013). doi:10.1103/PhysRevLett.110.182302. arXiv:1212.5198
32. D. d'Enterria et al., Constraints from the first LHC data on hadronic event generators for ultra-high energy cosmic-ray physics. Astropart. Phys. **35**, 98 (2011). doi:10.1016/j.astropartphys.2011.05.002. arXiv:1101.5596
33. ALICE Collaboration, Centrality dependence of π, K, p production in Pb-Pb collisions at $\sqrt{s_{NN}}$ = 2.76 TeV. Phys. Rev. C **88**, 044910 (2013). doi:10.1103/PhysRevC.88.044910. arXiv:1303.0737
34. P. Braun-Munzinger, D. Magestro, K. Redlich, J. Stachel, Hadron production in Au–Au collisions at rhic. Phys. Lett. B **518**, 41 (2001). doi:10.1016/S0370-2693(01)01069-3. arXiv:hep-ph/0105229
35. T. Sjöstrand, S. Mrenna, P. Z. Skands, PYTHIA 6.4 physics and manual. JHEP **05**, 026 (2006). doi:10.1088/1126-6708/2006/05/026. arXiv:hep-ph/0603175
36. J.E. Elias et al., Experimental study of multiparticle production in hadron-nucleus interactions at high energy. Phys. Rev. D **22**, 13 (1980). doi:10.1103/PhysRevD.22.13

The CMS Collaboration

Yerevan Physics Institute, Yerevan, Armenia
S. Chatrchyan, V. Khachatryan, A. M. Sirunyan, A. Tumasyan

Institut für Hochenergiephysik der OeAW, Wien, Austria
W. Adam, T. Bergauer, M. Dragicevic, J. Erö, C. Fabjan[1], M. Friedl, R. Frühwirth[1], V. M. Ghete, N. Hörmann, J. Hrubec, M. Jeitler[1], W. Kiesenhofer, V. Knünz, M. Krammer[1], I. Krätschmer, D. Liko, I. Mikulec, D. Rabady[2], B. Rahbaran, C. Rohringer, H. Rohringer, R. Schöfbeck, J. Strauss, A. Taurok, W. Treberer-Treberspurg, W. Waltenberger, C.-E. Wulz[1]

National Centre for Particle and High Energy Physics, Minsk, Belarus
V. Mossolov, N. Shumeiko, J. Suarez Gonzalez

Universiteit Antwerpen, Antwerpen, Belgium
S. Alderweireldt, M. Bansal, S. Bansal, T. Cornelis, E. A. De Wolf, X. Janssen, A. Knutsson, S. Luyckx, L. Mucibello, S. Ochesanu, B. Roland, R. Rougny, Z. Staykova, H. Van Haevermaet, P. Van Mechelen, N. Van Remortel, A. Van Spilbeeck

Vrije Universiteit Brussel, Brussel, Belgium
F. Blekman, S. Blyweert, J. D'Hondt, A. Kalogeropoulos, J. Keaveney, M. Maes, A. Olbrechts, S. Tavernier, W. Van Doninck, P. Van Mulders, G. P. Van Onsem, I. Villella

Université Libre de Bruxelles, Bruxelles, Belgium
C. Caillol, B. Clerbaux, G. De Lentdecker, L. Favart, A. P. R. Gay, T. Hreus, A. Léonard, P. E. Marage, A. Mohammadi, L. Perniè, T. Reis, T. Seva, L. Thomas, C. Vander Velde, P. Vanlaer, J. Wang

Ghent University, Ghent, Belgium
V. Adler, K. Beernaert, L. Benucci, A. Cimmino, S. Costantini, S. Dildick, G. Garcia, B. Klein, J. Lellouch, A. Marinov, J. Mccartin, A. A. Ocampo Rios, D. Ryckbosch, M. Sigamani, N. Strobbe, F. Thyssen, M. Tytgat, S. Walsh, E. Yazgan, N. Zaganidis

Université Catholique de Louvain, Louvain-la-Neuve, Belgium
S. Basegmez, C. Beluffi[3], G. Bruno, R. Castello, A. Caudron, L. Ceard, C. Delaere, T. du Pree, D. Favart, L. Forthomme, A. Giammanco[4], J. Hollar, P. Jez, V. Lemaitre, J. Liao, O. Militaru, C. Nuttens, D. Pagano, A. Pin, K. Piotrzkowski, A. Popov[5], M. Selvaggi, J. M. Vizan Garcia

Université de Mons, Mons, Belgium
N. Beliy, T. Caebergs, E. Daubie, G. H. Hammad

Centro Brasileiro de Pesquisas Fisicas, Rio de Janeiro, Brazil
G. A. Alves, M. Correa Martins Junior, T. Martins, M. E. Pol, M. H. G. Souza

Universidade do Estado do Rio de Janeiro, Rio de Janeiro, Brazil
W. L. Aldá Júnior, W. Carvalho, J. Chinellato[6], A. Custódio, E. M. Da Costa, D. De Jesus Damiao, C. De Oliveira Martins, S. Fonseca De Souza, H. Malbouisson, M. Malek, D. Matos Figueiredo, L. Mundim, H. Nogima, W. L. Prado Da Silva, A. Santoro, A. Sznajder, E. J. Tonelli Manganote[6], A. Vilela Pereira

Universidade Estadual Paulista, São Paulo, Brazil
F. A. Dias[7], T. R. Fernandez Perez Tomei, C. Lagana, S. F. Novaes, Sandra S. Padula

Universidade Federal do ABC, São Paulo, Brazil
C. A. Bernardes, E. M. Gregores, P. G. Mercadante

Institute for Nuclear Research and Nuclear Energy, Sofia, Bulgaria
V. Genchev[2], P. Iaydjiev[2], S. Piperov, M. Rodozov, G. Sultanov, M. Vutova

University of Sofia, Sofia, Bulgaria
A. Dimitrov, R. Hadjiiska, V. Kozhuharov, L. Litov, B. Pavlov, P. Petkov

Institute of High Energy Physics, Beijing, China
J. G. Bian, G. M. Chen, H. S. Chen, C. H. Jiang, D. Liang, S. Liang, X. Meng, J. Tao, J. Wang, X. Wang, Z. Wang, H. Xiao, M. Xu

State Key Laboratory of Nuclear Physics and Technology,Peking University, Beijing, China
C. Asawatangtrakuldee, Y. Ban, Y. Guo, W. Li, S. Liu, Y. Mao, S. J. Qian, H. Teng, D. Wang, L. Zhang, W. Zou

Universidad de Los Andes, Bogota, Colombia
C. Avila, C. A. Carrillo Montoya, L. F. Chaparro Sierra, J. P. Gomez, B. Gomez Moreno, J. C. Sanabria

Technical University of Split, Split, Croatia
N. Godinovic, D. Lelas, R. Plestina[8], D. Polic, I. Puljak

University of Split, Split, Croatia
Z. Antunovic, M. Kovac

Institute Rudjer Boskovics, Zagreb, Croatia
V. Brigljevic, S. Duric, K. Kadija, J. Luetic, D. Mekterovic, S. Morovic, L. Tikvica

University of Cyprus, Nicosia, Cyprus
A. Attikis, G. Mavromanolakis, J. Mousa, C. Nicolaou, F. Ptochos, P. A. Razis

Charles University, Prague, Czech Republic
M. Finger, M. Finger Jr.

Academy of Scientific Research and Technology of the Arab Republic of Egypt, Egyptian Network of High Energy Physics, Cairo, Egypt
A. A. Abdelalim[9], Y. Assran[10], S. Elgammal[9], A. Ellithi Kamel[11], M. A. Mahmoud[12], A. Radi[13,14]

National Institute of Chemical Physics and Biophysics, Tallinn, Estonia
M. Kadastik, M. Müntel, M. Murumaa, M. Raidal, L. Rebane, A. Tiko

Department of Physics, University of Helsinki, Helsinki, Finland
P. Eerola, G. Fedi, M. Voutilainen

Helsinki Institute of Physics, Helsinki, Finland
J. Härkönen, V. Karimäki, R. Kinnunen, M. J. Kortelainen, T. Lampén, K. Lassila-Perini, S. Lehti, T. Lindén, P. Luukka, T. Mäenpää, T. Peltola, E. Tuominen, J. Tuominiemi, E. Tuovinen, L. Wendland

Lappeenranta University of Technology, Lappeenranta, Finland
T. Tuuva

DSM/IRFU, CEA/Saclay, Gif-sur-Yvette, France
M. Besancon, F. Couderc, M. Dejardin, D. Denegri, B. Fabbro, J. L. Faure, F. Ferri, S. Ganjour, A. Givernaud, P. Gras, G. Hamel de Monchenault, P. Jarry, E. Locci, J. Malcles, L. Millischer, A. Nayak, J. Rander, A. Rosowsky, M. Titov

Laboratoire Leprince-Ringuet, Ecole Polytechnique, IN2P3-CNRS, Palaiseau, France
S. Baffioni, F. Beaudette, L. Benhabib, M. Bluj[15], P. Busson, C. Charlot, N. Daci, T. Dahms, M. Dalchenko, L. Dobrzynski, A. Florent, R. Granier de Cassagnac, M. Haguenauer, P. Miné, C. Mironov, I. N. Naranjo, M. Nguyen, C. Ochando, P. Paganini, D. Sabes, R. Salerno, Y. Sirois, C. Veelken, A. Zabi

Institut Pluridisciplinaire Hubert Curien Université de Strasbourg, Université de Haute Alsace Mulhouse, CNRS/IN2P3, Strasbourg, France
J.-L. Agram[16], J. Andrea, D. Bloch, J.-M. Brom, E. C. Chabert, C. Collard, E. Conte[16], F. Drouhin[16], J.-C. Fontaine[16], D. Gelé, U. Goerlach, C. Goetzmann, P. Juillot, A.-C. Le Bihan, P. Van Hove

Centre de Calcul de l'Institut National de Physique Nucleaire et de Physique des Particules, CNRS/IN2P3, Villeurbanne, France
S. Gadrat

Université de Lyon, Université Claude Bernard Lyon 1, CNRS-IN2P3, Institut de Physique Nucléaire de Lyon, Villeurbanne, France
S. Beauceron, N. Beaupere, G. Boudoul, S. Brochet, J. Chasserat, R. Chierici, D. Contardo, P. Depasse, H. El Mamouni, J. Fay, S. Gascon, M. Gouzevitch, B. Ille, T. Kurca, M. Lethuillier, L. Mirabito, S. Perries, L. Sgandurra, V. Sordini, M. Vander Donckt, P. Verdier, S. Viret

Institute of High Energy Physics and Informatization, Tbilisi State University, Tbilisi, Georgia
Z. Tsamalaidze[17]

RWTH Aachen University, I. Physikalisches Institut, Aachen, Germany
C. Autermann, S. Beranek, B. Calpas, M. Edelhoff, L. Feld, N. Heracleous, O. Hindrichs, K. Klein, A. Ostapchuk, A. Perieanu, F. Raupach, J. Sammet, S. Schael, D. Sprenger, H. Weber, B. Wittmer, V. Zhukov[5]

RWTH Aachen University, III. Physikalisches Institut A, Aachen, Germany
M. Ata, J. Caudron, E. Dietz-Laursonn, D. Duchardt, M. Erdmann, R. Fischer, A. Güth, T. Hebbeker, C. Heidemann, K. Hoepfner, D. Klingebiel, P. Kreuzer, M. Merschmeyer, A. Meyer, M. Olschewski, K. Padeken, P. Papacz, H. Pieta, H. Reithler, S. A. Schmitz, L. Sonnenschein, J. Steggemann, D. Teyssier, S. Thüer, M. Weber

RWTH Aachen University, III. Physikalisches Institut B, Aachen, Germany
V. Cherepanov, Y. Erdogan, G. Flügge, H. Geenen, M. Geisler, W. Haj Ahmad, F. Hoehle, B. Kargoll, T. Kress, Y. Kuessel, J. Lingemann[2], A. Nowack, I. M. Nugent, L. Perchalla, O. Pooth, A. Stahl

Deutsches Elektronen-Synchrotron, Hamburg, Germany
M. Aldaya Martin, I. Asin, N. Bartosik, J. Behr, W. Behrenhoff, U. Behrens, M. Bergholz[18], A. Bethani, K. Borras, A. Burgmeier, A. Cakir, L. Calligaris, A. Campbell, S. Choudhury, F. Costanza, C. Diez Pardos, S. Dooling, T. Dorland,

G. Eckerlin, D. Eckstein, G. Flucke, A. Geiser, I. Glushkov, P. Gunnellini, S. Habib, J. Hauk, G. Hellwig, D. Horton, H. Jung, M. Kasemann, P. Katsas, C. Kleinwort, H. Kluge, M. Krämer, D. Krücker, E. Kuznetsova, W. Lange, J. Leonard, K. Lipka, W. Lohmann[18], B. Lutz, R. Mankel, I. Marfin, I.-A. Melzer-Pellmann, A. B. Meyer, J. Mnich, A. Mussgiller, S. Naumann-Emme, O. Novgorodova, F. Nowak, J. Olzem, H. Perrey, A. Petrukhin, D. Pitzl, R. Placakyte, A. Raspereza, P. M. Ribeiro Cipriano, C. Riedl, E. Ron, M. Ö. Sahin, J. Salfeld-Nebgen, R. Schmidt[18], T. Schoerner-Sadenius, N. Sen, M. Stein, R. Walsh, C. Wissing

University of Hamburg, Hamburg, Germany
V. Blobel, H. Enderle, J. Erfle, E. Garutti, U. Gebbert, M. Görner, M. Gosselink, J. Haller, K. Heine, R. S. Höing, G. Kaussen, H. Kirschenmann, R. Klanner, R. Kogler, J. Lange, I. Marchesini, T. Peiffer, N. Pietsch, D. Rathjens, C. Sander, H. Schettler, P. Schleper, E. Schlieckau, A. Schmidt, M. Schröder, T. Schum, M. Seidel, J. Sibille[19], V. Sola, H. Stadie, G. Steinbrück, J. Thomsen, D. Troendle, E. Usai, L. Vanelderen

Institut für Experimentelle Kernphysik, Karlsruhe, Germany
C. Barth, C. Baus, J. Berger, C. Böser, E. Butz, T. Chwalek, W. De Boer, A. Descroix, A. Dierlamm, M. Feindt, M. Guthoff[2], F. Hartmann[2], T. Hauth[2], H. Held, K. H. Hoffmann, U. Husemann, I. Katkov[5], J. R. Komaragiri, A. Kornmayer[2], P. Lobelle Pardo, D. Martschei, Th. Müller, M. Niegel, A. Nürnberg, O. Oberst, J. Ott, G. Quast, K. Rabbertz, F. Ratnikov, S. Röcker, F.-P. Schilling, G. Schott, H. J. Simonis, F. M. Stober, R. Ulrich, J. Wagner-Kuhr, S. Wayand, T. Weiler, M. Zeise

Institute of Nuclear and Particle Physics (INPP), NCSR Demokritos, Aghia Paraskevi, Greece
G. Anagnostou, G. Daskalakis, T. Geralis, S. Kesisoglou, A. Kyriakis, D. Loukas, A. Markou, C. Markou, E. Ntomari

University of Athens, Athens, Greece
L. Gouskos, A. Panagiotou, N. Saoulidou, E. Stiliaris

University of Ioánnina, Ioánnina, Greece
X. Aslanoglou, I. Evangelou, G. Flouris, C. Foudas, P. Kokkas, N. Manthos, I. Papadopoulos, E. Paradas

KFKI Research Institute for Particle and Nuclear Physics, Budapest, Hungary
G. Bencze, C. Hajdu, P. Hidas, D. Horvath[20], F. Sikler, V. Veszpremi, G. Vesztergombi[21], A. J. Zsigmond

Institute of Nuclear Research ATOMKI, Debrecen, Hungary
N. Beni, S. Czellar, J. Molnar, J. Palinkas, Z. Szillasi

University of Debrecen, Debrecen, Hungary
J. Karancsi, P. Raics, Z. L. Trocsanyi, B. Ujvari

National Institute of Science Education and Research, Bhubaneswar, India
S. K. Swain[22]

Panjab University, Chandigarh, India
S. B. Beri, V. Bhatnagar, N. Dhingra, R. Gupta, M. Kaur, M. Z. Mehta, M. Mittal, N. Nishu, L. K. Saini, A. Sharma, J. B. Singh

University of Delhi, Delhi, India
Ashok Kumar, Arun Kumar, S. Ahuja, A. Bhardwaj, B. C. Choudhary, S. Malhotra, M. Naimuddin, K. Ranjan, P. Saxena, V. Sharma, R. K. Shivpuri

Saha Institute of Nuclear Physics, Kolkata, India
S. Banerjee, S. Bhattacharya, K. Chatterjee , S. Dutta, B. Gomber, Sa. Jain, Sh. Jain, R. Khurana, A. Modak, S. Mukherjee, D. Roy, S. Sarkar, M. Sharan

Bhabha Atomic Research Centre, Mumbai, India
A. Abdulsalam, D. Dutta, S. Kailas, V. Kumar, A. K. Mohanty[2], L. M. Pant, P. Shukla, A. Topkar

Tata Institute of Fundamental Research - EHEP, Mumbai, India
T. Aziz, R. M. Chatterjee, S. Ganguly, S. Ghosh, M. Guchait[23], A. Gurtu[24], G. Kole, S. Kumar, M. Maity[25], G. Majumder, K. Mazumdar, G. B. Mohanty, B. Parida, K. Sudhakar, N. Wickramage[26]

Tata Institute of Fundamental Research - HECR, Mumbai, India
S. Banerjee, S. Dugad

Institute for Research in Fundamental Sciences (IPM), Tehran, Iran
H. Arfaei, H. Bakhshiansohi, S. M. Etesami[27], A. Fahim[28], A. Jafari, M. Khakzad, M. Mohammadi Najafabadi, S. Paktinat Mehdiabadi, B. Safarzadeh[29], M. Zeinali

University College Dublin, Dublin, Ireland
M. Grunewald

INFN Sezione di Bari, Bari, Italy
M. Abbrescia, L. Barbone, C. Calabria, S. S. Chhibra, A. Colaleo, D. Creanza, N. De Filippis, M. De Palma, L. Fiore, G. Iaselli, G. Maggi, M. Maggi, B. Marangelli, S. My, S. Nuzzo, N. Pacifico, A. Pompili, G. Pugliese, G. Selvaggi, L. Silvestris, G. Singh, R. Venditti, P. Verwilligen, G. Zito

Università di Bari, Bari, Italy
M. Abbrescia, L. Barbone, C. Calabria, S. S. Chhibra, M. De Palma, B. Marangelli, S. Nuzzo, A. Pompili, G. Selvaggi, G. Singh, R. Venditti

Politecnico di Bari, Bari, Italy
D. Creanza, N. De Filippis, G. Iaselli, G. Maggi, S. My, G. Pugliese

INFN Sezione di Bologna, Bologna, Italy
G. Abbiendi, A. C. Benvenuti, D. Bonacorsi, S. Braibant-Giacomelli, L. Brigliadori, R. Campanini, P. Capiluppi, A. Castro, F. R. Cavallo, G. Codispoti, M. Cuffiani, G. M. Dallavalle, F. Fabbri, A. Fanfani, D. Fasanella, P. Giacomelli, C. Grandi, L. Guiducci, S. Marcellini, G. Masetti, M. Meneghelli, A. Montanari, F. L. Navarria, F. Odorici, A. Perrotta, F. Primavera, A. M. Rossi, T. Rovelli, G. P. Siroli, N. Tosi, R. Travaglini

Università di Bologna, Bologna, Italy
D. Bonacorsi, S. Braibant-Giacomelli, L. Brigliadori, R. Campanini, P. Capiluppi, A. Castro, G. Codispoti, M. Cuffiani, A. Fanfani, D. Fasanella, L. Guiducci, M. Meneghelli, F. L. Navarria, F. Primavera, A. M. Rossi, T. Rovelli, G. P. Siroli, N. Tosi, R. Travaglini

INFN Sezione di Catania, Catania, Italy
S. Albergo, M. Chiorboli, S. Costa, F. Giordano[2], R. Potenza, A. Tricomi, C. Tuve

Università di Catania, Catania, Italy
S. Albergo, M. Chiorboli, S. Costa, R. Potenza, A. Tricomi, C. Tuve

INFN Sezione di Firenze, Firenze, Italy
G. Barbagli, V. Ciulli, C. Civinini, R. D'Alessandro, E. Focardi, S. Frosali, E. Gallo, S. Gonzi, V. Gori, P. Lenzi, M. Meschini, S. Paoletti, G. Sguazzoni, A. Tropiano

Università di Firenze, Firenze, Italy
V. Ciulli, R. D'Alessandro, E. Focardi, S. Frosali, S. Gonzi, V. Gori, P. Lenzi, A. Tropiano

INFN Laboratori Nazionali di Frascati, Frascati, Italy
L. Benussi, S. Bianco, F. Fabbri, D. Piccolo

INFN Sezione di Genova, Genova, Italy
P. Fabbricatore, R. Musenich, S. Tosi

Università di Genova, Genova, Italy
S. Tosi

INFN Sezione di Milano-Bicocca, Milano, Italy
A. Benaglia, F. De Guio, M. E. Dinardo, S. Fiorendi, S. Gennai, A. Ghezzi, P. Govoni, M. T. Lucchini[2], S. Malvezzi, R. A. Manzoni[2], A. Martelli[2], D. Menasce, L. Moroni, M. Paganoni, D. Pedrini, S. Ragazzi, N. Redaelli, T. Tabarelli de Fatis

Università di Milano-Bicocca, Milano, Italy
F. De Guio, M. E. Dinardo, S. Fiorendi, A. Ghezzi, P. Govoni, M. T. Lucchini[2], R. A. Manzoni[2], A. Martelli[2], M. Paganoni, S. Ragazzi, T. Tabarelli de Fatis

INFN Sezione di Napoli, Napoli, Italy
S. Buontempo, N. Cavallo, A. De Cosa, F. Fabozzi, A. O. M. Iorio, L. Lista, S. Meola[2], M. Merola, P. Paolucci[2]

Università di Napoli 'Federico II', Napoli, Italy
A. De Cosa, A. O. M. Iorio

Università della Basilicata (Potenza), Napoli, Italy
N. Cavallo, F. Fabozzi

Università G. Marconi (Roma), Napoli, Italy
S. Meola[2]

INFN Sezione di Padova, Padova, Italy
P. Azzi, N. Bacchetta, D. Bisello, A. Branca, R. Carlin, P. Checchia, T. Dorigo, U. Dosselli, M. Galanti[2], F. Gasparini, U. Gasparini, P. Giubilato, F. Gonella, A. Gozzelino, K. Kanishchev, S. Lacaprara, I. Lazzizzera, M. Margoni, A. T. Meneguzzo, F. Montecassiano, M. Passaseo, J. Pazzini, N. Pozzobon, P. Ronchese, F. Simonetto, E. Torassa, M. Tosi, S. Vanini, P. Zotto, A. Zucchetta, G. Zumerle

Università di Padova, Padova, Italy
D. Bisello, A. Branca, R. Carlin, M. Galanti[2], F. Gasparini, U. Gasparini, P. Giubilato, F. K. Kanishchev, I. Lazzizzera, M. Margoni, A. T. Meneguzzo, J. Pazzini, N. Pozzobon, P. Ronchese, F. Simonetto, M. Tosi, S. Vanini, P. Zotto, A. Zucchetta, G. Zumerle

Università di Trento (Trento), Padova, Italy
K. Kanishchev, I. Lazzizzera

INFN Sezione di Pavia, Pavia, Italy
M. Gabusi, S. P. Ratti, C. Riccardi, P. Vitulo

Università di Pavia, Pavia, Italy
M. Gabusi, S. P. Ratti, C. Riccardi, P. Vitulo

INFN Sezione di Perugia, Perugia, Italy
M Biasini, G. M. Bilei, L. Fanò, P. Lariccia, G. Mantovani, M. Menichelli, A. Nappi†, F. Romeo, A. Saha, A. Santocchia, A. Spiezia

Università di Perugia, Perugia, Italy
M Biasini, L Fanò, P Lariccia, G Mantovani, A Nappi†, F. Romeo, A Santocchia, A. Spiezia

INFN Sezione di Pisa, Pisa, Italy
K. Androsov[30], P. Azzurri, G. Bagliesi, J. Bernardini, T. Boccali, G. Broccolo, R. Castaldi, M. A. Ciocci, R. T. D'Agnolo[2], R. Dell'Orso, F. Fiori, L. Foà, A. Giassi, M. T. Grippo[30], A. Kraan, F. Ligabue, T. Lomtadze, L. Martini[30], A. Messineo, F. Palla, A. Rizzi, A. Savoy-Navarro[31], A. T. Serban, P. Spagnolo, P. Squillacioti, R. Tenchini, G. Tonelli, A. Venturi, P. G. Verdini, C. Vernieri

Università di Pisa, Pisa, Italy
A. Messineo, A. Rizzi, G. Tonelli

Scuola Normale Superiore di Pisa, Pisa, Italy
G. Broccolo, R. T. D'Agnolo[2], F. Fiori, L. Foà, F. Ligabue, C. Vernieri

INFN Sezione di Roma, Roma, Italy
L. Barone, F. Cavallari, D. Del Re, M. Diemoz, M. Grassi[2], E. Longo, F. Margaroli, P. Meridiani, F. Micheli, S. Nourbakhsh, G. Organtini, R. Paramatti, S. Rahatlou, C. Rovelli, L. Soffi

Università di Roma, Roma, Italy
L. Barone, D. Del Re, M. Grassi[2], E. Longo, F. Margaroli, F. Micheli, S. Nourbakhsh, G. Organtini , S. Rahatlou, C. Rovelli[32], L. Soffi

INFN Sezione di Torino, Torino, Italy
N. Amapane, R. Arcidiacono, S. Argiro, M. Arneodo, R. Bellan , C. Biino, N. Cartiglia, S. Casasso, M. Costa, N. Demaria , C. Mariotti, S. Maselli, G. Mazza, E. Migliore, V. Monaco , M. Musich, M. M. Obertino, N. Pastrone, M. Pelliccioni[2], A. Potenza, A. Romero, M. Ruspa, R. Sacchi, A. Solano, A. Staiano, U. Tamponi

Università di Torino, Torino, Italy
N. Amapane, S. Argiro, R. Bellan, S. Casasso, M. Costa , E. Migliore, V. Monaco, A. Potenza, A. Romero, R. Sacchi, A. Solano

Università del Piemonte Orientale (Novara), Torino, Italy
R. Arcidiacono, M. Arneodo, M. M. Obertino, M. Ruspa

INFN Sezione di Trieste, Trieste, Italy
S. Belforte, V. Candelise, M. Casarsa, F. Cossutti[2], G. Della Ricca, B. Gobbo, C. La Licata, M. Marone, D. Montanino, A. Penzo, A. Schizzi, A. Zanetti

Università di Trieste, Trieste, Italy
V. Candelise, G. Della Ricca, C. La Licata, M. Marone, D. Montanino, A. Schizzi

Kangwon National University, Chunchon, Korea
S. Chang, T. Y. Kim, S. K. Nam

Kyungpook National University, Daegu, Korea
D. H. Kim, G. N. Kim, J. E. Kim, D. J. Kong, Y. D. Oh, H. Park, D. C. Son

Institute for Universe and Elementary Particles, Chonnam National University, Kwangju, Korea
J. Y. Kim, Zero J. Kim, S. Song

Korea University, Seoul, Korea
S. Choi, D. Gyun, B. Hong, M. Jo, H. Kim, T. J. Kim, K. S. Lee, S. K. Park, Y. Roh

University of Seoul, Seoul, Korea
M. Choi, J. H. Kim, C. Park, I. C. Park, S. Park, G. Ryu

Sungkyunkwan University, Suwon, Korea
Y. Choi, Y. K. Choi, J. Goh, M. S. Kim, E. Kwon, B. Lee, J. Lee, S. Lee, H. Seo, I. Yu

Vilnius University, Vilnius, Lithuania
I. Grigelionis, A. Juodagalvis

Centro de Investigacion y de Estudios Avanzados del IPN, Mexico City, Mexico
H. Castilla-Valdez, E. De La Cruz-Burelo, I. Heredia de La Cruz[33], R. Lopez-Fernandez, J. Martínez-Ortega, A. Sanchez-Hernandez, L. M. Villasenor-Cendejas

Universidad Iberoamericana, Mexico City, Mexico
S. Carrillo Moreno, F. Vazquez Valencia

Benemerita Universidad Autonoma de Puebla, Puebla, Mexico
H. A. Salazar Ibarguen

Universidad Autónoma de San Luis Potosí, San Luis Potosí, Mexico
E. Casimiro Linares, A. Morelos Pineda, M. A. Reyes-Santos

University of Auckland, Auckland, New Zealand
D. Krofcheck

University of Canterbury, Christchurch, New Zealand
A. J. Bell, P. H. Butler, R. Doesburg, S. Reucroft, H. Silverwood

National Centre for Physics, Quaid-I-Azam University, Islamabad, Pakistan
M. Ahmad, M. I. Asghar, J. Butt, H. R. Hoorani, S. Khalid, W. A. Khan, T. Khurshid, S. Qazi, M. A. Shah, M. Shoaib

National Centre for Nuclear Research, Swierk, Poland
H. Bialkowska, B. Boimska, T. Frueboes, M. Górski, M. Kazana, K. Nawrocki, K. Romanowska-Rybinska, M. Szleper, G. Wrochna, P. Zalewski

Institute of Experimental Physics, Faculty of Physics, University of Warsaw, Warsaw, Poland
G. Brona, K. Bunkowski, M. Cwiok, W. Dominik, K. Doroba, A. Kalinowski, M. Konecki, J. Krolikowski, M. Misiura, W. Wolszczak

Laboratório de Instrumentação e Física Experimental de Partículas, Lisboa, Portugal
N. Almeida, P. Bargassa, C. Beirão Da Cruz E Silva, P. Faccioli, P. G. Ferreira Parracho, M. Gallinaro, F. Nguyen, J. Rodrigues Antunes, J. Seixas[2], J. Varela, P. Vischia

Joint Institute for Nuclear Research, Dubna, Russia
S. Afanasiev, P. Bunin, M. Gavrilenko, I. Golutvin, I. Gorbunov, V. Karjavin, V. Konoplyanikov, G. Kozlov, A. Lanev, A. Malakhov, V. Matveev, P. Moisenz, V. Palichik, V. Perelygin, S. Shmatov, N. Skatchkov, V. Smirnov, A. Zarubin

Petersburg Nuclear Physics Institute, Gatchina (St. Petersburg), Russia
S. Evstyukhin, V. Golovtsov, Y. Ivanov, V. Kim, P. Levchenko, V. Murzin, V. Oreshkin, I. Smirnov, V. Sulimov, L. Uvarov, S. Vavilov, A. Vorobyev, An. Vorobyev

Institute for Nuclear Research, Moscow, Russia
Yu. Andreev, A. Dermenev, S. Gninenko, N. Golubev, M. Kirsanov, N. Krasnikov, A. Pashenkov, D. Tlisov, A. Toropin

Institute for Theoretical and Experimental Physics, Moscow, Russia
V. Epshteyn, M. Erofeeva, V. Gavrilov, N. Lychkovskaya, V. Popov, G. Safronov, S. Semenov, A. Spiridonov, V. Stolin, E. Vlasov, A. Zhokin

P.N. Lebedev Physical Institute, Moscow, Russia
V. Andreev, M. Azarkin, I. Dremin, M. Kirakosyan, A. Leonidov, G. Mesyats, S. V. Rusakov, A. Vinogradov

Skobeltsyn Institute of Nuclear Physics, Lomonosov Moscow State University, Moscow, Russia
A. Belyaev, E. Boos, A. Ershov, A. Gribushin, V. Klyukhin, O. Kodolova, V. Korotkikh, I. Lokhtin, A. Markina, S. Obraztsov, S. Petrushanko, V. Savrin, A. Snigirev, I. Vardanyan

State Research Center of Russian Federation, Institute for High Energy Physics, Protvino, Russia
I. Azhgirey, I. Bayshev, S. Bitioukov, V. Kachanov, A. Kalinin, D. Konstantinov, V. Krychkine, V. Petrov, R. Ryutin, A. Sobol, L. Tourtchanovitch, S. Troshin, N. Tyurin, A. Uzunian, A. Volkov

University of Belgrade, Faculty of Physics and Vinca Institute of Nuclear Sciences, Belgrade, Serbia
P. Adzic[34], M. Djordjevic, M. Ekmedzic, D. Krpic[34], J. Milosevic

Centro de Investigaciones Energéticas Medioambientales y Tecnológicas (CIEMAT), Madrid, Spain
M. Aguilar-Benitez, J. Alcaraz Maestre, C. Battilana, E. Calvo, M. Cerrada, M. Chamizo Llatas[2], N. Colino, B. De La Cruz, A. Delgado Peris, D. Domínguez Vázquez, C. Fernandez Bedoya, J. P. Fernández Ramos, A. Ferrando, J. Flix, M. C. Fouz, P. Garcia-Abia, O. Gonzalez Lopez, S. Goy Lopez, J. M. Hernandez, M. I. Josa, G. Merino, E. Navarro De Martino, J. Puerta Pelayo, A. Quintario Olmeda, I. Redondo, L. Romero, J. Santaolalla, M. S. Soares, C. Willmott

Universidad Autónoma de Madrid, Madrid, Spain
C. Albajar, J. F. de Trocóniz

Universidad de Oviedo, Oviedo, Spain
H. Brun, J. Cuevas, J. Fernandez Menendez, S. Folgueras, I. Gonzalez Caballero, L. Lloret Iglesias, J. Piedra Gomez

Instituto de Física de Cantabria (IFCA), CSIC-Universidad de Cantabria, Santander, Spain
J. A. Brochero Cifuentes, I. J. Cabrillo, A. Calderon, S. H. Chuang, J. Duarte Campderros, M. Fernandez, G. Gomez, J. Gonzalez Sanchez, A. Graziano, C. Jorda, A. Lopez Virto, J. Marco, R. Marco, C. Martinez Rivero, F. Matorras, F. J. Munoz Sanchez, T. Rodrigo, A. Y. Rodríguez-Marrero, A. Ruiz-Jimeno, L. Scodellaro, I. Vila, R. Vilar Cortabitarte

CERN, European Organization for Nuclear Research, Geneva, Switzerland
D. Abbaneo, E. Auffray, G. Auzinger, M. Bachtis, P. Baillon, A. H. Ball, D. Barney, J. Bendavid, J. F. Benitez, C. Bernet[8], G. Bianchi, P. Bloch, A. Bocci, A. Bonato, O. Bondu, C. Botta, H. Breuker, T. Camporesi, G. Cerminara, T. Christiansen, J. A. Coarasa Perez, S. Colafranceschi[35], D. d'Enterria, A. Dabrowski, A. David, A. De Roeck, S. De Visscher, S. Di Guida, M. Dobson, N. Dupont-Sagorin, A. Elliott-Peisert, J. Eugster, W. Funk, G. Georgiou, M. Giffels, D. Gigi, K. Gill, D. Giordano, M. Girone, M. Giunta, F. Glege, R. Gomez-Reino Garrido, S. Gowdy, R. Guida, J. Hammer, M. Hansen, P. Harris, C. Hartl, A. Hinzmann, V. Innocente, P. Janot, E. Karavakis, K. Kousouris, K. Krajczar, P. Lecoq, Y. -J. Lee, C. Lourenço, N. Magini, M. Malberti, L. Malgeri, M. Mannelli, L. Masetti, F. Meijers, S. Mersi, E. Meschi, R. Moser, M. Mulders, P. Musella, E. Nesvold, L. Orsini, E. Palencia Cortezon, E. Perez, L. Perrozzi, A. Petrilli, A. Pfeiffer, M. Pierini, M. Pimiä, D. Piparo, M. Plagge, L. Quertenmont, A. Racz, W. Reece, G. Rolandi[36], M. Rovere, H. Sakulin, F. Santanastasio, C. Schäfer, C. Schwick, I. Segoni, S. Sekmen, A. Sharma, P. Siegrist, P. Silva, M. Simon, P. Sphicas[37], D. Spiga, M. Stoye, A. Tsirou, G. I. Veres[21], J. R. Vlimant, H. K. Wöhri, S. D. Worm[38], W. D. Zeuner

Paul Scherrer Institut, Villigen, Switzerland
W. Bertl, K. Deiters, W. Erdmann, K. Gabathuler, R. Horisberger, Q. Ingram, H. C. Kaestli, S. König, D. Kotlinski, U. Langenegger, D. Renker, T. Rohe

Institute for Particle Physics, ETH Zurich, Zurich, Switzerland
F. Bachmair, L. Bäni, L. Bianchini, P. Bortignon, M. A. Buchmann, B. Casal, N. Chanon, A. Deisher, G. Dissertori, M. Dittmar, M. Donegà, M. Dünser, P. Eller, K. Freudenreich, C. Grab, D. Hits, P. Lecomte, W. Lustermann, B. Mangano, A. C. Marini, P. Martinez Ruiz del Arbol, D. Meister, N. Mohr, F. Moortgat, C. Nägeli[39], P. Nef, F. Nessi-Tedaldi, F. Pandolfi, L. Pape, F. Pauss, M. Peruzzi, F. J. Ronga, M. Rossini, L. Sala, A. K. Sanchez, A. Starodumov[40], B. Stieger, M. Takahashi, L. Tauscher†, A. Thea, K. Theofilatos, D. Treille, C. Urscheler, R. Wallny, H. A. Weber

Universität Zürich, Zurich, Switzerland
C. Amsler[41], V. Chiochia, C. Favaro, M. Ivova Rikova, B. Kilminster, B. Millan Mejias, P. Otiougova, P. Robmann, H. Snoek, S. Taroni, S. Tupputi, M. Verzetti

National Central University, Chung-Li, Taiwan
M. Cardaci, K. H. Chen, C. Ferro, C. M. Kuo, S. W. Li, W. Lin, Y. J. Lu, R. Volpe, S. S. Yu

National Taiwan University (NTU), Taipei, Taiwan
P. Bartalini, P. Chang, Y. H. Chang, Y. W. Chang, Y. Chao, K. F. Chen, C. Dietz, U. Grundler, W.-S. Hou, Y. Hsiung, K. Y. Kao, Y. J. Lei, R.-S. Lu, D. Majumder, E. Petrakou, X. Shi, J. G. Shiu, Y. M. Tzeng, M. Wang

Chulalongkorn University, Bangkok, Thailand
B. Asavapibhop, N. Suwonjandee

Cukurova University, Adana, Turkey
A. Adiguzel, M. N. Bakirci[42], S. Cerci[43], C. Dozen, I. Dumanoglu, E. Eskut, S. Girgis, G. Gokbulut, E. Gurpinar, I. Hos, E. E. Kangal, A. Kayis Topaksu, G. Onengut[44], K. Ozdemir, S. Ozturk[42], A. Polatoz, K. Sogut[45], D. Sunar Cerci[43], B. Tali[43], H. Topakli[42], M. Vergili

Physics Department, Middle East Technical University, Ankara, Turkey
I. V. Akin, T. Aliev, B. Bilin, S. Bilmis, M. Deniz, H. Gamsizkan, A. M. Guler, G. Karapinar[46], K. Ocalan, A. Ozpineci, M. Serin, R. Sever, U. E. Surat, M. Yalvac, M. Zeyrek

Bogazici University, Istanbul, Turkey
E. Gülmez, B. Isildak[47], M. Kaya[48], O. Kaya[48], S. Ozkorucuklu[49], N. Sonmez[50]

Istanbul Technical University, Istanbul, Turkey
H. Bahtiyar[51], E. Barlas, K. Cankocak, Y. O. Günaydin[52], F. I. Vardarlı, M. Yücel

National Scientific Center, Kharkov Institute of Physics and Technology, Kharkov, Ukraine
L. Levchuk, P. Sorokin

University of Bristol, Bristol, UK
J. J. Brooke, E. Clement, D. Cussans, H. Flacher, R. Frazier, J. Goldstein, M. Grimes, G. P. Heath, H. F. Heath, L. Kreczko, S. Metson, D. M. Newbold[38], K. Nirunpong, A. Poll, S. Senkin, V. J. Smith, T. Williams

Rutherford Appleton Laboratory, Didcot, UK
A. Belyaev[53], C. Brew, R. M. Brown, D. J. A. Cockerill, J. A. Coughlan, K. Harder, S. Harper, E. Olaiya, D. Petyt, B. C. Radburn-Smith, C. H. Shepherd-Themistocleous, I. R. Tomalin, W. J. Womersley

Imperial College, London, UK
R. Bainbridge, O. Buchmuller, D. Burton, D. Colling, N. Cripps, M. Cutajar, P. Dauncey, G. Davies, M. Della Negra, W. Ferguson, J. Fulcher, D. Futyan, A. Gilbert, A. Guneratne Bryer, G. Hall, Z. Hatherell, J. Hays, G. Iles, M. Jarvis, G. Karapostoli, M. Kenzie, R. Lane, R. Lucas[38], L. Lyons, A. -M. Magnan, J. Marrouche, B. Mathias, R. Nandi, J. Nash, A. Nikitenko[40], J. Pela, M. Pesaresi, K. Petridis, M. Pioppi[54], D. M. Raymond, S. Rogerson, A. Rose, C. Seez, P. Sharp†, A. Sparrow, A. Tapper, M. Vazquez Acosta, T. Virdee, S. Wakefield, N. Wardle, T. Whyntie

Brunel University, Uxbridge, UK
M. Chadwick, J. E. Cole, P. R. Hobson, A. Khan, P. Kyberd, D. Leggat, D. Leslie, W. Martin, I. D. Reid, P. Symonds, L. Teodorescu, M. Turner

Baylor University, Waco, USA
J. Dittmann, K. Hatakeyama, A. Kasmi, H. Liu, T. Scarborough

The University of Alabama, Tuscaloosa, USA
O. Charaf, S. I. Cooper, C. Henderson, P. Rumerio

Boston University, Boston, USA
A. Avetisyan, T. Bose, C. Fantasia, A. Heister, P. Lawson, D. Lazic, J. Rohlf, D. Sperka, J. St. John, L. Sulak

Brown University, Providence, USA
J. Alimena, S. Bhattacharya, G. Christopher, D. Cutts, Z. Demiragli, A. Ferapontov, A. Garabedian, U. Heintz, S. Jabeen, G. Kukartsev, E. Laird, G. Landsberg, M. Luk, M. Narain, M. Segala, T. Sinthuprasith, T. Speer

University of California, Davis, USA
R. Breedon, G. Breto, M. Calderon De La Barca Sanchez, S. Chauhan, M. Chertok, J. Conway, R. Conway, P. T. Cox, R. Erbacher, M. Gardner, R. Houtz, W. Ko, A. Kopecky, R. Lander, T. Miceli, D. Pellett, F. Ricci-Tam, B. Rutherford, M. Searle, J. Smith, M. Squires, M. Tripathi, S. Wilbur, R. Yohay

University of California, Los Angeles, USA
V. Andreev, D. Cline, R. Cousins, S. Erhan, P. Everaerts, C. Farrell, M. Felcini, J. Hauser, M. Ignatenko, C. Jarvis, G. Rakness, P. Schlein†, E. Takasugi, P. Traczyk, V. Valuev, M. Weber

University of California, Riverside, USA
J. Babb, R. Clare, J. Ellison, J. W. Gary, G. Hanson, P. Jandir, H. Liu, O. R. Long, A. Luthra, H. Nguyen, S. Paramesvaran, J. Sturdy, S. Sumowidagdo, R. Wilken, S. Wimpenny

University of California, San Diego, La Jolla, USA
W. Andrews, J. G. Branson, G. B. Cerati, S. Cittolin, D. Evans, A. Holzner, R. Kelley, M. Lebourgeois, J. Letts, I. Macneill, S. Padhi, C. Palmer, G. Petrucciani, M. Pieri, M. Sani, V. Sharma, S. Simon, E. Sudano, M. Tadel, Y. Tu, A. Vartak, S. Wasserbaech[55], F. Würthwein, A. Yagil, J. Yoo

University of California, Santa Barbara, Santa Barbara, USA
D. Barge, C. Campagnari, M. D'Alfonso, T. Danielson, K. Flowers, P. Geffert, C. George, F. Golf , J. Incandela, C. Justus, P. Kalavase, D. Kovalskyi, V. Krutelyov, S. Lowette, R. Magaña Villalba, N. Mccoll, V. Pavlunin, J. Ribnik, J. Richman, R. Rossin, D. Stuart, W. To , C. West

California Institute of Technology, Pasadena, USA
A. Apresyan, A. Bornheim, J. Bunn, Y. Chen, E. Di Marco , J. Duarte, D. Kcira, Y. Ma, A. Mott, H. B. Newman, C. Rogan, M. Spiropulu, V. Timciuc, J. Veverka, R. Wilkinson, S. Xie, Y. Yang, R. Y. Zhu

Carnegie Mellon University, Pittsburgh, USA
V. Azzolini, A. Calamba, R. Carroll, T. Ferguson, Y. Iiyama, D. W. Jang, Y. F. Liu, M. Paulini, J. Russ, H. Vogel, I. Vorobiev

University of Colorado at Boulder, Boulder, USA
J. P. Cumalat, B. R. Drell, W. T. Ford, A. Gaz, E. Luiggi Lopez, U. Nauenberg, J. G. Smith, K. Stenson, K. A. Ulmer, S. R. Wagner

Cornell University, Ithaca, USA
J. Alexander, A. Chatterjee, N. Eggert, L. K. Gibbons, W. Hopkins, A. Khukhunaishvili, B. Kreis , N. Mirman, G. Nicolas Kaufman, J. R. Patterson, A. Ryd, E. Salvati, W. Sun, W. D. Teo, J. Thom, J. Thompson, J. Tucker, Y. Weng, L. Winstrom, P. Wittich

Fairfield University, Fairfield, USA
D. Winn

Fermi National Accelerator Laboratory, Batavia, USA
S. Abdullin, M. Albrow, J. Anderson, G. Apollinari, L. A. T. Bauerdick, A. Beretvas , J. Berryhill, P. C. Bhat, K. Burkett, J. N. Butler, V. Chetluru, H. W. K. Cheung, F. Chlebana, S. Cihangir, V. D. Elvira, I. Fisk, J. Freeman, Y. Gao, E. Gottschalk, L. Gray, D. Green, O. Gutsche, D. Hare, R. M. Harris, J. Hirschauer, B. Hooberman, S. Jindariani, M. Johnson, U. Joshi, K. Kaadze, B. Klima, S. Kunori, S. Kwan, J. Linacre, D. Lincoln, R. Lipton, J. Lykken, K. Maeshima, J. M. Marraffino, V. I. Martinez Outschoorn, S. Maruyama, D. Mason, P. McBride, K. Mishra, S. Mrenna, Y. Musienko[56], C. Newman-Holmes, V. O'Dell, O. Prokofyev, N. Ratnikova, E. Sexton-Kennedy, S. Sharma, W. J. Spalding, L. Spiegel, L. Taylor, S. Tkaczyk, N. V. Tran, L. Uplegger, E. W. Vaandering, R. Vidal, J. Whitmore, W. Wu, F. Yang, J. C. Yun

University of Florida, Gainesville, USA
D. Acosta, P. Avery, D. Bourilkov, M. Chen, T. Cheng, S. Das, M. De Gruttola, G. P. Di Giovanni, D. Dobur, A. Drozdetskiy, R. D. Field, M. Fisher, Y. Fu, I. K. Furic, J. Hugon, B. Kim, J. Konigsberg, A. Korytov, A. Kropivnitskaya, T. Kypreos, J. F. Low, K. Matchev, P. Milenovic[57], G. Mitselmakher, L. Muniz, R. Remington, A. Rinkevicius, N. Skhirtladze, M. Snowball, J. Yelton, M. Zakaria

Florida International University, Miami, USA
V. Gaultney, S. Hewamanage, S. Linn, P. Markowitz, G. Martinez, J. L. Rodriguez

Florida State University, Tallahassee, USA
T. Adams, A. Askew, J. Bochenek, J. Chen, B. Diamond, S. V. Gleyzer, J. Haas, S. Hagopian, V. Hagopian, K. F. Johnson, H. Prosper, V. Veeraraghavan, M. Weinberg

Florida Institute of Technology, Melbourne, USA
M. M. Baarmand, B. Dorney, M. Hohlmann, H. Kalakhety, F. Yumiceva

University of Illinois at Chicago (UIC), Chicago, USA
M. R. Adams, L. Apanasevich, V. E. Bazterra , R. R. Betts, I. Bucinskaite, J. Callner, R. Cavanaugh, O. Evdokimov, L. Gauthier, C. E. Gerber, D. J. Hofman, S. Khalatyan, P. Kurt, F. Lacroix, D. H. Moon, C. O'Brien, C. Silkworth, D. Strom, P. Turner, N. Varelas

The University of Iowa, Iowa City, USA
U. Akgun, E. A. Albayrak[51], B. Bilki[58], W. Clarida, K. Dilsiz, F. Duru, S. Griffiths, J.-P. Merlo, H. Mermerkaya[59], A. Mestvirishvili, A. Moeller, J. Nachtman, C. R. Newsom, H. Ogul, Y. Onel, F. Ozok[51], S. Sen, P. Tan, E. Tiras, J. Wetzel, T. Yetkin[60], K. Yi

Johns Hopkins University, Baltimore, USA
B. A. Barnett, B. Blumenfeld, S. Bolognesi, G. Giurgiu, A. V. Gritsan, G. Hu, P. Maksimovic, C. Martin, M. Swartz, A. Whitbeck

The University of Kansas, Lawrence, USA
P. Baringer, A. Bean, G. Benelli, R. P. Kenny III, M. Murray, D. Noonan, S. Sanders, R. Stringer, J. S. Wood

Kansas State University, Manhattan, USA
A. F. Barfuss, I. Chakaberia, A. Ivanov, S. Khalil, M. Makouski, Y. Maravin, S. Shrestha, I. Svintradze

Lawrence Livermore National Laboratory, Livermore, USA
J. Gronberg, D. Lange, F. Rebassoo, D. Wright

University of Maryland, College Park, USA
A. Baden, B. Calvert, S. C. Eno, J. A. Gomez, N. J. Hadley, R. G. Kellogg, T. Kolberg, Y. Lu, M. Marionneau, A. C. Mignerey, K. Pedro, A. Peterman, A. Skuja, J. Temple, M. B. Tonjes, S. C. Tonwar

Massachusetts Institute of Technology, Cambridge, USA
A. Apyan, G. Bauer, W. Busza, I. A. Cali, M. Chan, L. Di Matteo, V. Dutta, G. Gomez Ceballos, M. Goncharov, D. Gulhan, Y. Kim, M. Klute, Y. S. Lai, A. Levin, P. D. Luckey, T. Ma, S. Nahn, C. Paus, D. Ralph, C. Roland, G. Roland, G. S. F. Stephans, F. Stöckli, K. Sumorok, D. Velicanu, R. Wolf, B. Wyslouch, M. Yang, Y. Yilmaz, A. S. Yoon, M. Zanetti, V. Zhukova

University of Minnesota, Minneapolis, USA
B. Dahmes, A. De Benedetti, G. Franzoni, A. Gude, J. Haupt, S. C. Kao, K. Klapoetke, Y. Kubota, J. Mans, N. Pastika, R. Rusack, M. Sasseville, A. Singovsky, N. Tambe, J. Turkewitz

University of Mississippi, Oxford, USA
J. G. Acosta, L. M. Cremaldi, R. Kroeger, S. Oliveros, L. Perera, R. Rahmat, D. A. Sanders, D. Summers

University of Nebraska-Lincoln, Lincoln, USA
E. Avdeeva, K. Bloom, S. Bose, D. R. Claes, A. Dominguez, M. Eads, R. Gonzalez Suarez, J. Keller, I. Kravchenko, J. Lazo-Flores, S. Malik, F. Meier, G. R. Snow

State University of New York at Buffalo, Buffalo, USA
J. Dolen, A. Godshalk, I. Iashvili, S. Jain, A. Kharchilava, A. Kumar, S. Rappoccio, Z. Wan

Northeastern University, Boston, USA
G. Alverson, E. Barberis, D. Baumgartel, M. Chasco, J. Haley, A. Massironi, D. Nash, T. Orimoto, D. Trocino, D. Wood, J. Zhang

Northwestern University, Evanston, USA
A. Anastassov, K. A. Hahn, A. Kubik, L. Lusito, N. Mucia, N. Odell, B. Pollack, A. Pozdnyakov, M. Schmitt, S. Stoynev, K. Sung, M. Velasco, S. Won

University of Notre Dame, Notre Dame, USA
D. Berry, A. Brinkerhoff, K. M. Chan, M. Hildreth, C. Jessop, D. J. Karmgard, J. Kolb, K. Lannon, W. Luo, S. Lynch, N. Marinelli, D. M. Morse, T. Pearson, M. Planer, R. Ruchti, J. Slaunwhite, N. Valls, M. Wayne, M. Wolf

The Ohio State University, Columbus, USA
L. Antonelli, B. Bylsma, L. S. Durkin, C. Hill, R. Hughes, K. Kotov, T. Y. Ling, D. Puigh, M. Rodenburg, G. Smith, C. Vuosalo, B. L. Winer, H. Wolfe

Princeton University, Princeton, USA
E. Berry, P. Elmer, V. Halyo, P. Hebda, J. Hegeman, A. Hunt, P. Jindal, S. A. Koay, P. Lujan, D. Marlow, T. Medvedeva, M. Mooney, J. Olsen, P. Piroué, X. Quan, A. Raval, H. Saka, D. Stickland, C. Tully, J. S. Werner, S. C. Zenz, A. Zuranski

University of Puerto Rico, Mayaguez, USA
E. Brownson, A. Lopez, H. Mendez, J. E. Ramirez Vargas

Purdue University, West Lafayette, USA
E. Alagoz, D. Benedetti, G. Bolla, D. Bortoletto, M. De Mattia, A. Everett, Z. Hu, M. Jones, K. Jung, O. Koybasi, M. Kress, N. Leonardo, D. Lopes Pegna, V. Maroussov, P. Merkel, D. H. Miller, N. Neumeister, I. Shipsey, D. Silvers, A. Svyatkovskiy, M. Vidal Marono, F. Wang, W. Xie, L. Xu, H. D. Yoo, J. Zablocki, Y. Zheng

Purdue University Calumet, Hammond, USA
S. Guragain, N. Parashar

Rice University, Houston, USA
A. Adair, B. Akgun, K. M. Ecklund, F. J. M. Geurts, W. Li, B. P. Padley, R. Redjimi, J. Roberts, J. Zabel

University of Rochester, Rochester, USA
B. Betchart, A. Bodek, R. Covarelli, P. de Barbaro, R. Demina, Y. Eshaq, T. Ferbel, A. Garcia-Bellido, P. Goldenzweig, J. Han, A. Harel, D. C. Miner, G. Petrillo, D. Vishnevskiy, M. Zielinski

The Rockefeller University, New York, USA
A. Bhatti, R. Ciesielski, L. Demortier, K. Goulianos, G. Lungu, S. Malik, C. Mesropian

Rutgers, The State University of New Jersey, Piscataway, USA
S. Arora, A. Barker, J. P. Chou, C. Contreras-Campana, E. Contreras-Campana, D. Duggan, D. Ferencek, Y. Gershtein, R. Gray, E. Halkiadakis, D. Hidas, A. Lath, S. Panwalkar, M. Park, R. Patel, V. Rekovic, J. Robles, S. Salur, S. Schnetzer, C. Seitz, S. Somalwar, R. Stone, S. Thomas, P. Thomassen, M. Walker

University of Tennessee, Knoxville, USA
G. Cerizza, M. Hollingsworth, K. Rose, S. Spanier, Z. C. Yang, A. York

Texas A&M University, College Station, USA
O. Bouhali[61], R. Eusebi, W. Flanagan, J. Gilmore, T. Kamon[62], V. Khotilovich, R. Montalvo, I. Osipenkov, Y. Pakhotin, A. Perloff, J. Roe, A. Safonov, T. Sakuma, I. Suarez, A. Tatarinov, D. Toback

Texas Tech University, Lubbock, USA
N. Akchurin, C. Cowden, J. Damgov, C. Dragoiu, P. R. Dudero, C. Jeong, K. Kovitanggoon, S. W. Lee, T. Libeiro, I. Volobouev

Vanderbilt University, Nashville, USA
E. Appelt, A. G. Delannoy, S. Greene, A. Gurrola, W. Johns, C. Maguire, Y. Mao, A. Melo, M. Sharma, P. Sheldon, B. Snook, S. Tuo, J. Velkovska

University of Virginia, Charlottesville, USA
M. W. Arenton, S. Boutle, B. Cox, B. Francis, J. Goodell, R. Hirosky, A. Ledovskoy, C. Lin, C. Neu, J. Wood

Wayne State University, Detroit, USA
S. Gollapinni, R. Harr, P. E. Karchin, C. Kottachchi Kankanamge Don, P. Lamichhane, A. Sakharov

University of Wisconsin, Madison, USA
D. A. Belknap, L. Borrello, D. Carlsmith, M. Cepeda, S. Dasu, E. Friis, M. Grothe, R. Hall-Wilton, M. Herndon, A. Hervé, P. Klabbers, J. Klukas, A. Lanaro, R. Loveless, A. Mohapatra, M. U. Mozer, I. Ojalvo, G. A. Pierro, G. Polese, I. Ross, A. Savin, W. H. Smith, J. Swanson

† **Deceased**

1: Also at Vienna University of Technology, Vienna, Austria
2: Also at CERN, European Organization for Nuclear Research, Geneva, Switzerland
3: Also at Institut Pluridisciplinaire Hubert Curien, Université de Strasbourg, Université de Haute Alsace Mulhouse, CNRS/IN2P3, Strasbourg, France
4: Also at National Institute of Chemical Physics and Biophysics, Tallinn, Estonia
5: Also at Skobeltsyn Institute of Nuclear Physics, Lomonosov Moscow State University, Moscow, Russia
6: Also at Universidade Estadual de Campinas, Campinas, Brazil
7: Also at California Institute of Technology, Pasadena, USA
8: Also at Laboratoire Leprince-Ringuet, Ecole Polytechnique, IN2P3-CNRS, Palaiseau, France
9: Also at Zewail City of Science and Technology, Zewail, Egypt
10: Also at Suez Canal University, Suez, Egypt
11: Also at Cairo University, Cairo, Egypt
12: Also at Fayoum University, El-Fayoum, Egypt
13: Also at British University in Egypt, Cairo, Egypt
14: Now at Ain Shams University, Cairo, Egypt
15: Also at National Centre for Nuclear Research, Swierk, Poland
16: Also at Université de Haute Alsace, Mulhouse, France
17: Also at Joint Institute for Nuclear Research, Dubna, Russia

18: Also at Brandenburg University of Technology, Cottbus, Germany
19: Also at The University of Kansas, Lawrence, USA
20: Also at Institute of Nuclear Research ATOMKI, Debrecen, Hungary
21: Also at Eötvös Loránd University, Budapest, Hungary
22: Also at Tata Institute of Fundamental Research - EHEP, Mumbai, India
23: Also at Tata Institute of Fundamental Research - HECR, Mumbai, India
24: Now at King Abdulaziz University, Jeddah, Saudi Arabia
25: Also at University of Visva-Bharati, Santiniketan, India
26: Also at University of Ruhuna, Matara, Sri Lanka
27: Also at Isfahan University of Technology, Isfahan, Iran
28: Also at Sharif University of Technology, Tehran, Iran
29: Also at Plasma Physics Research Center, Science and Research Branch, Islamic Azad University, Tehran, Iran
30: Also at Università degli Studi di Siena, Siena, Italy
31: Also at Purdue University, West Lafayette, USA
32: Also at INFN Sezione di Roma, Roma, Italy
33: Also at Universidad Michoacana de San Nicolas de Hidalgo, Morelia, Mexico
34: Also at Faculty of Physics, University of Belgrade, Belgrade, Serbia
35: Also at Facoltà Ingegneria, Università di Roma, Roma, Italy
36: Also at Scuola Normale e Sezione dell'INFN, Pisa, Italy
37: Also at University of Athens, Athens, Greece
38: Also at Rutherford Appleton Laboratory, Didcot, UK
39: Also at Paul Scherrer Institut, Villigen, Switzerland
40: Also at Institute for Theoretical and Experimental Physics, Moscow, Russia
41: Also at Albert Einstein Center for Fundamental Physics, Bern, Switzerland
42: Also at Gaziosmanpasa University, Tokat, Turkey
43: Also at Adiyaman University, Adiyaman, Turkey
44: Also at Cag University, Mersin, Turkey
45: Also at Mersin University, Mersin, Turkey
46: Also at Izmir Institute of Technology, Izmir, Turkey
47: Also at Ozyegin University, Istanbul, Turkey
48: Also at Kafkas University, Kars, Turkey
49: Also at Suleyman Demirel University, Isparta, Turkey
50: Also at Ege University, Izmir, Turkey
51: Also at Mimar Sinan University, Istanbul, Istanbul, Turkey
52: Also at Kahramanmaras Sütcü Imam University, Kahramanmaras, Turkey
53: Also at School of Physics and Astronomy, University of Southampton, Southampton, UK
54: Also at INFN Sezione di Perugia, Università di Perugia, Perugia, Italy
55: Also at Utah Valley University, Orem, USA
56: Also at Institute for Nuclear Research, Moscow, Russia
57: Also at University of Belgrade, Faculty of Physics and Vinca Institute of Nuclear Sciences, Belgrade, Serbia
58: Also at Argonne National Laboratory, Argonne, USA
59: Also at Erzincan University, Erzincan, Turkey
60: Also at Yildiz Technical University, Istanbul, Turkey
61: Also at Texas A&M University at Qatar, Doha, Qatar
62: Also at Kyungpook National University, Daegu, Korea